ISTANBUL TECHNICAL UNIVERSITY ★ GRADUATE SCHOOL

STRUCTURAL HEALTH MONITORING USING FREQUENCY SELECTIVE SURFACE AS A PASSIVE SENSOR

M.Sc. THESIS

Mona MAKTABİ BAŞOĞLU

Department of Communication Systems

Satellite Communication and Remote Sensing Programme

FEBRUARY 2021

ISTANBUL TECHNICAL UNIVERSITY ★ GRADUATE SCHOOL

STRUCTURAL HEALTH MONITORING USING FREQUENCY SELECTIVE SURFACE AS A PASSIVE SENSOR

M.Sc. THESIS

Mona MAKTABİ BAŞOĞLU
(705171029)

Department of Communication Systems

Satellite Communication and Remote Sensing Program

Thesis Advisor: Prof. Dr. Sedef KENT PINAR
Thesis Co-Advisor: Dr. Bora DÖKEN

FEBRUARY 2021

İSTANBUL TEKNİK ÜNİVERSİTESİ ★ LİSANSÜSTÜ EĞİTİM ENSTİTÜSÜ

YAPISAL SAĞLIK İZLEMEDE FREKANS SEÇİCİ YÜZEYLERİN KULLANILMASI

YÜKSEK LİSANS TEZİ

Mona MAKTABİ BAŞOĞLU
(705171029)

İletişim Sistemleri Anabilim Dalı

Uydu Haberleşme ve Uzaktan Algılama Programı

Tez Danışmanı: Prof. Dr. Sedef KENT PINAR
Eş Danışman: Dr. Bora DÖKEN

ŞUBAT 2021

Mona MAKTABİ BAŞOĞLU, a M.Sc. student of ITU Informatics Institute student ID 705171029, successfully defended the thesis entitled "STRUCTURAL HEALTH MONITORING USING FREQUENCY SELECTIVE SURFACES AS A PASSIVE SENSOR", which she prepared after fulfilling the requirements specified in the associated legislations, before the jury whose signatures are below.

Thesis Advisor :	**Prof. Dr. Sedef KENT PINAR** Istanbul Technical University	....
Co-advisor :	**Dr. Bora DÖKEN** Istanbul Technical University	....
Jury Members :	**Prof. Dr. Mesut KARTAL** Istanbul Technical University	....
	Assoc. Prof. Hamit TORPİ Yıldız Technical University	....
	Assoc. Prof. Serdar KARGIN Beykent University	....

Date of Submission : 22 January 2021
Date of Defense : 13 February 2021

To my husband and my profs,

FOREWORD

I would like to thank my adisors, Prof. Dr. Sedef Kent Pınar and Dr. Bora Döken for supporting me throughout my Master Degree. I am very gratful for Dr. Bora Döken for his guidance and continuous support throughout my thesis, through this journey he didn’t hesitate for a second to help me and share with me invaluable informations that without his help I wouldn’t reach here.

I would like to thank my husband and my family for being by myside with their limitless support and encourgment throughout my journey.

FEB 2021 Mona MAKTABİ BAŞOĞLU

TABLE OF CONTENTS

ABBREVIATIONS

FSS	:	Frequency Selective Surface
SHM	:	Structural Health Montoring
TE	:	Transverse Electric Waves
TM	:	Transverse Magnetic Waves
HFSS	:	High Frequncy Structure Simulator
E_i	:	Incident Plane Wave
E_t	:	Transmitted Plane Wave
E_r	:	Reflected Plane Wave
S_{21}	:	Transmission Coefficient
S_{11}	:	Reflected Coefficient
λ	:	Wavelength of incoming wave in free-space
g	:	Distance Between conductors
A, G	:	Correction Functions
Z_0	:	Characteristic Impedance
w	:	Conductive Strips Thickness
ω	:	Angular Frequency
BW	:	Bandwidth
RCS	:	Radar Cross Section
RF	:	Radio Frequency

LIST OF TABLES

Page

LIST OF FIGURES

Page

STRUCTURAL HEALTH MONITORING USING FREQUENCY SELECTIVE SURFACE AS A PASSIVE FILTER

SUMMARY

Structural health monitoring (SHM) is widely applied in various engineering sectors due to its ability in detecting damages, measuring deformation, pressure and temperature of a structure, while they can also provide information about the performance of these structures. Despite the fact that SHM can be applied with wire systems or wirelessly, nowadays SHM relies mainly on sensors that can be placed or mounted on any structure and can be monitored over time either in a passive or active way. Passive sensors are more likely to be used because they are affordable, can be easily installed and mounted on a structure, and they don't require any active element which as a result will live longer. One of the latest investigated sensors in SHM is using Frequency Selective Surfaces (FSSs) as a passive sensor. FSS with its geometric dependency can be very effective in detecting deformations in a civil structure. This can be understood form the frequency response of an FSS, where it is going to be altered after a deformation occur.

In this thesis, FSSs are used to design a passive sensor to detect tilting and cracking in civil structures. Two novel FSS geometries are proposed in this work. The first design is for detecting tilting angles, the new element geometry is capable of detecting deviation in civil structures with a linear frequency response change in the reflected mode this ensures that when any civil structures that have an FSS passive sensor mounted on it, its frequency response will be altered and change linearly with the same amount of deviation the structure was exposed to, and the second design is to detect cracking in civil structures, where the new element geometry is capable of detecting crack occurs along two axis at the same time, the results show that even when the thickness of the crack changes the frequency response will slightly change, and at the same time comparing the frequency response between before and after cracking we can see that the frequency response is shifted with almost 1 GHz.

Ansoft HFSS v.15 software is used for analyzing the electromagnetic behavior of FSS.

YAPISAL SAĞLIK İZLEMEDE FREKANS SEÇİCİ YÜZEYLERİN KULLANILMASI

ÖZET

Yapısal sağlık izleme (SHM), hasarları ve deformasyonları tespit etme kabiliyeti nedeniyle çeşitli mühendislik sektörlerinde yaygın olarak uygulanmaktadır. Bu hasarlar, normal veya kesme gerinim hasarları, sivil yapıların eğilmesi ve katmanlı yapılarda delaminasyondur. Bu, yapının yaşı, yanlış bir yapım süreci ve belki de çevresel bir sebep gibi birçok iç ve dış nedenden dolayı olabilir. Bu, Yapısal sağlık izlemeyi bir yapının kalan ömrünü tahmin etmedeki önemi için gerekli kılar veya örneğin bir deprem meydana geldiğinde SHM, hasarın büyüklüğünü kaydetmek için yapılar için hızlı analizler yapmak için kullanılabilir. Ülkeler, Yapısal sağlık izlemeyi geliştirmek için çok çaba, zaman ve para harcıyor. Malzemelerin mekaniği veya malzemelerin mukavemeti, yapıdaki deformasyonla ve yük altında oluşan gerilmeyle ilgilenir, burada bu yapının davranışını inceler ve kirişler, kolonlar ve şaftlar gibi yapısal elemanlardaki gerilmeleri ve gerilmeleri hesaplar . Dikkat edilmesi gereken en önemli parametrelerden biri yapı elemanı geometrisi ve özellikleridir, uzunluk, derinlik, genişlik ve ani değişikliklerin farklı anlamlara sahip olabileceği yerlerde dikkate alınmalıdır.

Herhangi bir malzeme birçok faktörden dolayı bazı değişikliklere maruz kalabilir; bu faktörler temel olarak normal şekil değiştirme, kayma gerilmesi, kolon burkulması ve delaminasyon olarak kategorize edilebilir. Bugün araştırmacılar, SHM'de kullanmak için sensörler geliştiriyor. SHM'de kullanılan algılayıcılar (sensorler) temelde aktif ve pasif olarak ikiye ayrılmaktadır. Pasif algılayıcılar uygun maliyetli olmaları, kolaylıkla monte edilebilmeleri ve sonuç olarak daha uzun ömürlü olmaları sebebiyle tercih edilmektedirler. Frekans seçici yüzeylerin (FSY) SHM'de pasif algılayıcı olarak kullanımı günümüzdeki önemli araştırma konularından biri olmaya başlamıştır.

FSY'ler dielektrik tabakalar üzerine basılmış düzlemsel periyodik iletken yapılardır. Gelen elektromanyetik dalgalar FSY'in iletken geometrileri üzerinde akım üretirken, iletkenler arasındaki iletken olmayan boşluklar üzerinde de bir elektrik alan üretilir. FSY'lerin periyodik iletken yapıları endüktans gibi davranırken, iletkenler arasındaki dielektrik boşluk kapasite gibi davranacaktır. Dolayısıyla, FSY'ler uzamsal filtre davranışı sergilerler. Frekans tepkileri, periyodik iletken geometrilerine, üzerine yazdırıldıkları dielektrik tabakaların elektriksel özelliklerine ve gelen elektromanyetik dalgaların frekans ve geliş açısına bağlıdır. FSY algılayıcının üzerine monte edildiği yapıda bir deformasyon meydana geldiğinde FSY'nin frekans cevabı da değişecektir. Frekans cevabındaki değişiklik sivil yapıdaki hasar miktarını verecektir.

Bu çalışmada, iki tane tasarım, biri çift daire şekilli geometriye dayanan yeni bir FSY geometrisi, ikincisi ise çapraz şekilli geometriye dayanan yeni bir FSY geometrisi

önerilmiştir. Önerilen birinci FSY geometrisi, sivil yapılarda meydana gelebilecek yana yatma hasarını algılayabilmektedir, bu yeni eleman geometrisi, doğrusal bir frekans tepkisi değişikliği ile sivil yapılardaki sapmayı tespit edebilir, bu, üzerine monte edilmiş bir FSS pasif sensörüne sahip herhangi bir inşaat yapısının, frekans yanıtının değiştirilmesini ve yapının maruz kaldığı aynı miktarda sapma ile doğrusal olarak değişmesini sağlar. Buradaki amacımız, yapımızın hangi açıdan saptığını anlamamız için FSS'nin olay açısını değiştirirken tepkisinin doğrusal olması gereken sivil yapılarda eğilmeyi tespit etmektir.

Bazı FSS tasarımlarının olay açısı değişimi için kararsız bir frekans tepkisine sahip olduğu kabul edilir, ancak bu bizim için yeterli değildir. Amacımız, yapı doğrusal bir şekilde saparken kararsız bir frekans tepkisine sahip olmaktır.

Dairesel döngü elemanları minyatürize edilmiş küçük elemanlardır ve örneğin dipol elemanla karşılaştırıldığında iyi ve kararlı bir frekans tepkisine sahiptirler, ancak aynı zamanda dipol elemanlarını da düşünürsek, boyut olarak çok büyük olacaklar ve büyük bir dizi olacaktır. FSS'mizi yapının küçük bir alanına monte etmek yerine, büyük elemanlar kullanırsak daha geniş bir alanı kaplamak zorunda kalacağımız durumumuzda bir dezavantaj olabilir. Bu pratik bir çözüm değil; bu nedenle dairesel elemanlar daha uygundur.

Ayrıca, sadece olay açısına duyarlılığı düşünmediğimizden ve doğrusallığın bizim durumumuz için çok kritik bir faktör olduğu durumlarda, frekans yanıtının değişiminin doğrusal olmasını istediğimizden.

Bu nedenle, örneğin, üçlü, çift kutuplu, çapraz çift kutuplu elemanlar, olay açısı değişikliğine karşı daha iyi bir hassasiyete sahip olabilir, ancak bükülmüş (dairesel) elemanların yapacağı gibi doğrusal bir performans vermeyecektir.

Çift halkalı döngü FSS tasarımının kullanılmasının nedeni, hem iç hem de dış döngü endüktansının tek daireli döngü ile aynı şekilde çalışmasıdır.

Diğer önemli şey, iç döngünün ikinci bir S21 yaratmasıdır, bu nedenle iki rezonans arasında dar bir S11 oluşturur. Ayrıca, iki komşu iç döngü geometrisi arasındaki mesafe oldukça büyük hale gelir. Bu nedenle ikinci S21 rezonansının açı kararlılığı oldukça düşüktür. Bu durum, S11 rezonansının düşük açı stabilitesine neden olur, burada aradığımız hedef budur. Ayrıca tasarımda dairesel geometriler kullanıldığı için rezonans frekansında ani sapmalar oluşmaz. Küçük açılı yapılardaki değişikliği fark etmemizi sağlamak için birim hücre geometrileri arasındaki mesafe büyük olacak şekilde düzenlenmiştir. Bununla birlikte, elemanlar arası mesafeyi arttırdığımızda aralarındaki kapasite değeri azalmaktadır. Bu durumda iletken yolların oluşturduğu eşdeğer endüktans değeri rezonansı belirler. Bu nedenle, dairesel bir döngü seçmenin ana nedeni, frekans yanıtının doğrusal olarak değişmesidir.

İkinci FSY geometrisi, sivil yapılarda meydana gelebilecek çatlamak hasarını algılayabilmektedir, rezonans frekansının, yapıdaki bir gerinim varlığında FSS elemanının etkin uzunluk artışı ile değiştirileceği yer. Ayrıca, yapı hasar gördüğünde, yapısal hasardan kaynaklanan çatlaklar FSS elemanının uzunluğunu kesebilir ve boşluk bırakabilir. Bu yeni eleman geometrisinin bir eksen boyunca oluşan çatlağı tespit edebilir iki eksen boyunca aynı anda iki eksen boyunca, sonuçlar, çatlağın kalınlığı değiştiğinde bile frekans yanıtının biraz değişeceğini ve aynı zamanda çatlama öncesi ve sonrası arasındaki frekans yanıtını karşılaştırdığımızda, frekans yanıtının değiştiğini neredeyse 1 GHz görebiliriz. Ek olarak, önerilen iki tasarım bir inşaat yapısında basılabilir ve test edilebilir ve sonuçlar gelecekteki çalışmalarda temsil edilen simülasyonlarla karşılaştırılabilir.

FSY'nin çalışma frekansı olarak S-bandı seçilmiştir. Daha düşük frekanslarda daha az dielektrik kayıp gerçekleştilmektedir ve ayrıca ölçülmesi daha kolay olduğundan ve çok maliyetli olmadığından dolayı S-bandı seçilmiştir. Ansoft HFSS v.15 yazılımı, FSS'nin elektromanyetik davranışını analiz etmek için kullanıldı.

1. INTRODUCTION

Structural Health Monitoring (SHM) is widely applied in many engineering sectors due to its importance in detecting damages in bridges, tunnels, and buildings. These damages are normal or shear strain damages, tilting of civil structures, and delamination in layered structures. This might happen due to many internal and external reasons such as, the age of the structure, an incorrect construction process, and maybe an environmental reason. Today, researchers are developing sensors to use in SHM. These sensors are mainly classified as active and passive sensors. Active sensors are more expensive and require more complex installations than passive sensor systems. Therefore, researchers focus on developing and improving passive sensors since they can be applied after the construction finishes.

One of the latest investigated sensors in SHM is to use frequency selective surfaces (FSSs) as passive sensors. FSSs are planar periodic conducting structures printed on dielectric substrates. Their frequency response is dependent on their periodic conducting geometries, the electrical properties of dielectric substrates that they are printed on, and the frequency and incident angle of the incoming electromagnetic waves. For that reason, when deformation occurs on a civil structure that FSS sensor mounted, the frequency response of FSS changes. The change in frequency response will give the amount of damage in the civil structure.

In this thesis, FSSs are used to design a passive sensor to detect tilting and cracking in civil structures. Two novel FSS geometries are proposed in this work. The first one is based on double circle shaped geometry is proposed to detect tilting in civil structure. The proposed FSS sensor detects tilting in angles civil structures. The propose of our design is to be able to detect and monitor any structural deviation based on the incident angle. Since the frequency response of FSS response depends on the angle of incoming electromagnetic waves, the tilting occurred in civil structures can be detected by the proposed FSS. The second which is based on crossed shaped geometry is for detecting crackings in civil structure. The working frequency of all designed FSS is chosen in S-band, since fewer dielectric losses are conducted in lower frequencies.

1.1 Purpose of Thesis

Structural health monitoring is a field attracted by many engineers and researchers in recent years, due to its importance in our life. SHM studies the structural health of infrastructure and detects any changes occur in the material or geometric properties of bridges, tunnels, and buildings. Many methods and approaches have been used and developed recently in this field. Despite the variety of existence and applied methods, sensors have preference over the other methods. Meanwhile, engineers and designers tend always to design a system with high performance and accurate data analysis, at the same time they work hard on reducing the complexity and the cost needed for a system. Therefore, this thesis proposes using FSS as a passive sensor in structural health monitoring applications. Since FSSs are highly sensitive to the incident angle and their response is quite dependent on their geometric formation, makes using them advantageous over the other sensors. For that reason, when a deformation will occur to the structure, FSS response for its geometric dependency will be altered and damage will be detected.

1.2 Literature Review

Since the beginning of the 20th century, the studies on periodic conductive patches or aperture arrays mounted on dielectric layer had been arisen. One of the earliest forms of periodic structures was the Frequency Selective Surfaces designed by Marconi and Franklin in 1919 [1]. However, their work started to gain potential in the middle of 1960s were the demand back then was highly rising in developing military applications. FSS started to be used in stealth technology for reducing the radar cross section RCS of communication systems, leading to diverse applications in antenna design, communication systems, satellite systems and many other applications. FSS can transmit nearly all electromagnetic waves, while also can reflect all energy through another frequency bandwidth. FSS's behavior depends on many factors such as their geometric and their response to incident angles. Because of the improvement studies in this field in analyzing complicated structures, this led the way to the introduction of numerous FSS models and their implementations, such as 3D FSS structures [2], active FSS [3], high-impedance surface absorbers [4], and fractal element FSS designs [5]. One of the latest of FSS structures is using them as passive sensors, in structural health monitoring applications. Lately, structural health monitoring is a very hot topic investigated by engineers and researchers due to its importance in our lives, where they have the ability to detect if the damage happened to an existing structure before it is too late. Many methods lately have been applied using different types of sensors and equipment to study these kinds of structural health monitoring. Some of them are wire systems, others are tending to improve wireless sensors systems for their easier installation and less complexity. Used sensors can be classified mainly into active and passive sensors, here in this thesis we are going to investigate using FSS as a passive sensor to detect the changes and damages which might occur to a structure.

2. FREQUENCY SELECTIVE SURFACE

In the recent years, an interesting area, named as Metasurface which are also called as planar Metamaterials with subwavelength thickness, has increasingly attracted attention to researchers due to their phenomenal abilities in light manipulation and versatility in ultrathin optical applications [6].

They are formed by periodic arrays in one, two- or three-dimensional array pattern. Usually, these arrays are metallic elements on a dielectric substrate. Many factors affect the electromagnetic properties of these arrays such as element geometry [7]. The subject of interest in this thesis, is Frequency Selective Surfaces FSSs, these metallic structures behave like inductors, while the dielectric gap between conductors will behave like capacitors. This means that the incident wave generates currents on the conducting elements, while an electric field is generated over the non-conducting gaps [1,8]. Frequency response of FSSs are dependent on the frequency and the incident angle of incident electromagnetic waves. Depending on their geometry, and since FSSs are made of metallic structures and they behave as capacitance and inductance towards incident waves, they have the ability to act as spatial filters. FSSs can be divided into low-pass, high-pass, band-stop and bandpass filters. Actually, all the periodic arrays can be excited in two ways, either by an incident plane wave E^i (Passive Array) or by individual generators connected to each element (Active Array). In the passive case, the incident plane wave is partly transmitted in the forward direction E^t and partly reflected in the specular direction E^r.

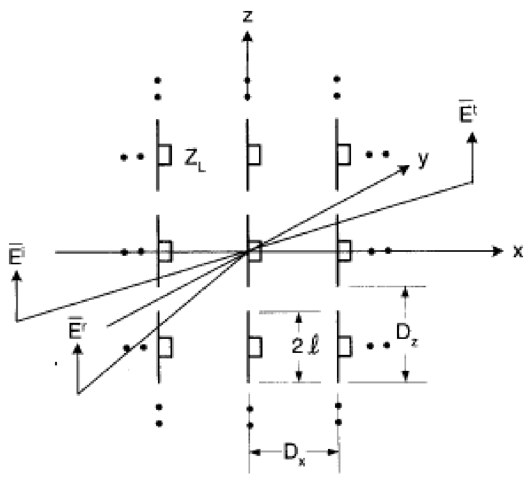

Figure 2.1: FSS excited by plane wave[1].

The reflection coefficient is equal to:

$$\Gamma = \frac{E^r}{E_i} \tag{2.1}$$

Similarly, the transmission coefficient could be defined as:

$$\tau = \frac{E^t}{E_i} \tag{2.2}$$

In general, FSS arrays can be classified as patch array and slot array. The only difference between patch (Figure2.2) array and slot array (Figure2.3) is that in patch arrays the electric currents are excited on the wires while in slot arrays the magnetic currents are excited in the slots where there is a voltage distribution in the slots [1]. Whereas, complementary arrays are accomplished by Basinet's principle, where it states that by arranging and slots arrays with elements of similar shape on the top of each other, this will result in a perfect conducting plane.

And the transmission coefficient for the complementary structure of one array is equal to the reflection coefficient for the array. For an array to operate perfectly, that their metallic thickness a dielectric substrate is very low. [1,9]

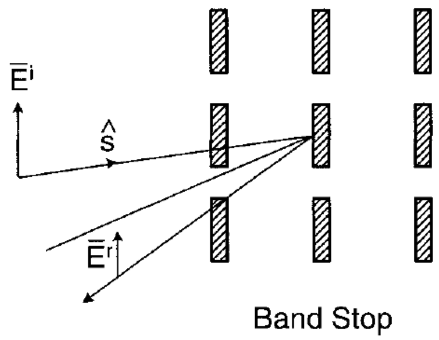

Figure 2.2 : Patch Array.

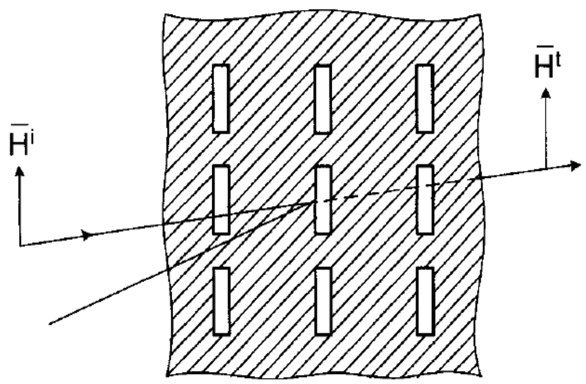

Figure 2.3 : Slot Array.

Also, adding a dielectric substrate changes the resonance frequency, because the dipole type will have a resonant frequency independent of the slab thickness, while the slot type will show a unit transmission at frequencies varying around $\frac{f_0}{\sqrt{e_r}}$ for symmetric dielectric slabs.

2.1 Applications of FSS

Periodic structures, specially frequency selective surfaces, have an abundant application over an immense range of the electromagnetic spectrum. The first potential application of FSS structures are radomes, they are used to reduce the radar cross section RCS of antenna outside their operational band, so it allows only the operational frequency to pass and reject the others frequencies outside the band as shown in Figure 2.4 [1].

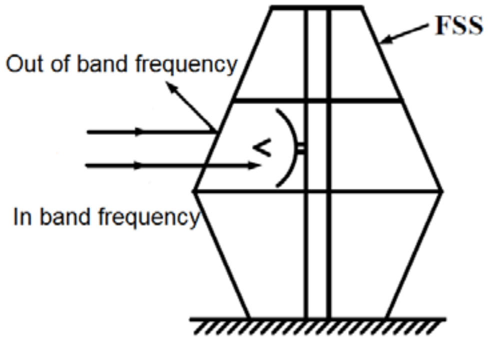

Figure 2.4 : Diagram of a radome [1].

FSSs have also been designed as sub and main reflectors in multiband reflector antennas as shown in Figure 2.5, FSS is transparent for the1st feed in the first operating band, while it operates as a sub-reflector in the second working frequency band for the 2nd feed antenna. [1,10].

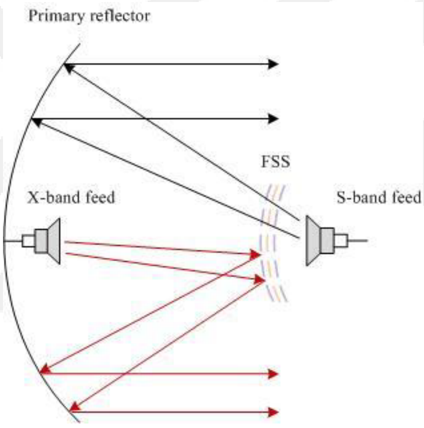

Figure 2.5 : Dual frequency reflector antenna with an FSS sub-reflector [5].

FSSs are also used in the civilian environment, hospitals schools etc., where they provide protection from harmful electromagnetic radiation especially in 2-3 GHz bands, they are used on the door of a Microwave ovens where they are made of a periodic array with metallic holes and designed to pass visible light (400 THz-700 THz) to enable seeing the food inside, while it reflects microwave radiation at 2.45 GHz [4].

FSSs are also been used in increasing the communication capabilities of the satellite. Another application of for FSSs is in wireless communications, where they have the ability to cut-off the unwanted radiation, this purpose is achieved by shielding floor and ceiling of FSS to prevent leakage of radio frequency. They also have applications in the near and far infrared regions, where it includes using polarizers, filters and beam splitters [11].

2.2 TYPES OF FSS

According to Munk [1], the most important part when designing either a band-pass or band-stop FSS is choosing the proper element. Some of them narrower-more banded or broader banded than the others, while some can be varied by design. These elements are a determinant of the resonant frequency, bandwidth, polarization response, and angular coverage of an FSS. Where adding a dielectric substrate to support the FSS can be essential in most array designs.

The element spacing have an impact on the bandwidth of any, where a small spacing will result in a wider bandwidth, and vice versa. In this case two things must be watched closely, earlier onset of grating lobes and greater variation of the first resonant frequency with angle of incidence and polarization. Therefore, a careful selection of element is essential.

These elements are classified into four categories, where each element type exhibiting its own frequency response characteristics. Those are center-connected or N-pole elements, loop elements, solid interior elements and combination elements.

2.2.1 The center connected

The center connected elements include, simple straight element, three-legged element; anchor elements; the Jerusalem cross; and the square spiral. An example of simple straight element, is Gangbuster surface, it consists of a simple straight dipole with an equal inter-element spacing.

Another example is the unloaded tripole array, the most important feature of about it, is that you can make the inter element spacing small and get a large bandwidth. The main disadvantages of unloaded tripole array and gangbuster, is that they suffer from excitation of the second harmonic for parallel polarization.

Anchor element are not more than a simple modification to the unloaded tripole, they are used to increase bandwidth and to add an end capacity. This does not only result in a larger bandwidth but also in much delayed inset of trapped as well as free space grating lobes. Ther is also Jerusalem cross, where it consists of two crossing dipoles which are loaded with small, orthogonal sections at their ends.

2.2.2 Loop types

The loop type elements include, three-and four-legged loaded elements; the circular loops; and the square hexagonal loops. These elements are mostly used in band-stop and band-pass applications.

Four-legged loaded elements, can be easily constructed using λ/2 with load impedance. for a greater bandwidth, stable incident angle and a better resonance, designing a small element is a good idea.

Hexagon elements provide a better and broad bandwidth in compare with four-legged elements, also they have a stable frequency response to incident angle changing.

2.2.3 Solid interior types

These elements were the earliest to be investigated, they are comprised of simple shapes such as squares, hexagons, circular disks. The element dimension is close to half a wavelength. These types of elements are used in limited applications, because the center frequency and bandwidth change in opposite sense for parallel and vertical polarizations as a function of incident angles.

2.2.4 Combination elements

These group of elements are constructed by combination of the other of the three group members to overcome the performance shortcomings (angular stability, bandwidth, and so on) and meet the demanded features of FSS structures.

2.3 Filters types and their geometries

The three most common types of filters are: strip grating filters, mesh filters, and cross-mesh filters. These classifications will help us to understand the physical background behind the working principle of FSS according to their geometrics.

2.3.1 Strip grating filters

This type of FSS filter is used to represent the theoretical concept of filters, where this is accomplished according to the incident wave direction with respect to the strip geometry. So, if the electric field of the incident wave is in the same direction of the strip length and is parallel to it, then we will have an inductive strip grating filter. Otherwise, if the incident wave is perpendicular to the strip length, then we will have a capacitive strip grating filter. Figure 2.6 explains the difference between the two cases of electric field direction [12].

Of course, since it is an incident wave and polarization dependence, this will limit the use of it, and because of that the only difference between capacitive and inductive situations is the polarization direction. So, these filters behave live lowpass and high pass filters.

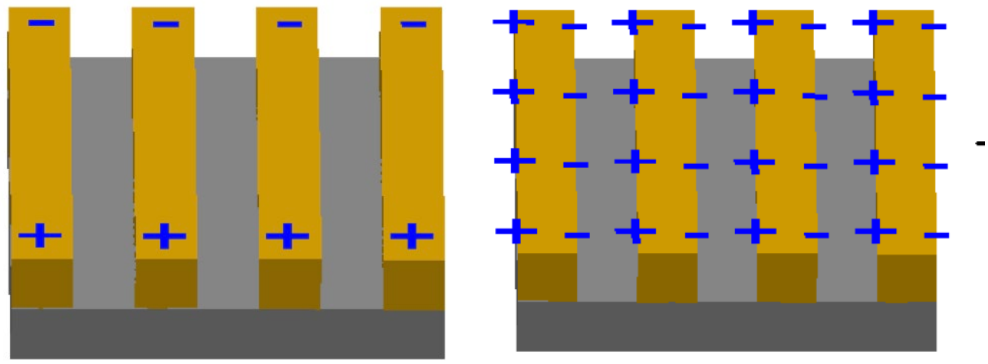

(a) (b)

Figure 2.6 : (a) Represents the inductive case where E-field is parallel, (b) represents the capacitive case where E-field is perpendicular.

2.3.2 Mesh filters

These filters (Figure 2.7) also act like lowpass and high pass filters, but the only difference between them and the strip filters is that they are designed in way which makes them independent of the incident wave and polarization direction.

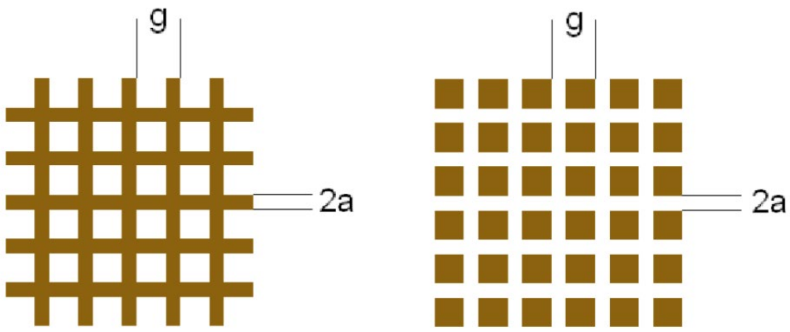

(a) (b)

Figure 2.7 : Representation of mesh filters, (a) represents inductive mesh filter and (b) represents capacitive mesh filter.

2.3.3 Cross-Mesh filters

These filters (Figure 2.8) are quite similar to mesh filters, except that they have a different shape, where mesh filters were represented as squares, unlike the cross-mesh filters are represented and modeled as a cross element. Resonant wavelength is determined by the dimensions of these elements [12].

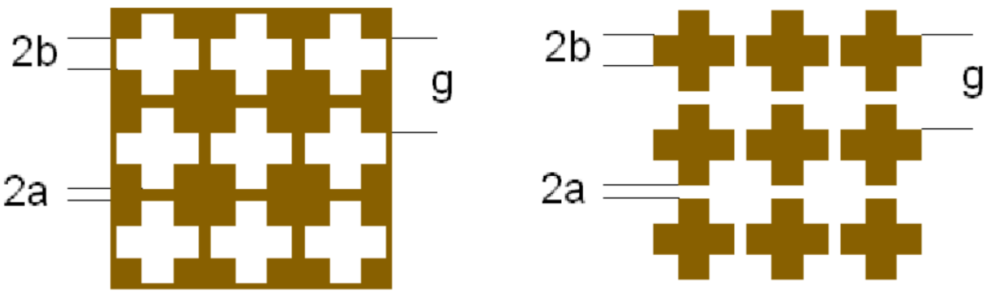

(a) (b)

Figure 2.0.8 : Representation of cross mesh filters, (a) represents inductive cross mesh filter and (b) represents captative cross mesh filter.

2.4 Key Properties of Designing FSS

There are many factors which they influence the frequency response and the performance of FSS. These factors are categorized into; Shape of the element, polarization and incident angle and effect of dielectric substrate.

2.4.1 Shape of the element

While designing, one of the most important factors that should be considered is the element geometry of FSS. A proper element selection must be done based on bandwidth, resonant frequency, incident angle and polarization response. So, depending on the geometry of the element, FSS can control the transmission and reflection of incident electromagnetic plane wave.

The resonant frequency response is determined by the element dimensions such as, separation period, dimension of the element, width of the element and inter element spacing. Table 2.1 summarizes the performance of different element shapes based on a single layer freestanding FSS. Ratings: best =1, second best =2,.....

Table 2.1 : Performance of FSS with different element shapes [8].

Element shape	Angular stability	Cross polarization level	Larger bandwidth	Small band separation
Dipole	4	1	4	1
Jerusalem Cross	2	3	2	2
Ring	1	2	1	1
Tripole	3	3	3	2
Cross Dipole	3	3	3	3
Square Loop	1	1	1	1

2.4.2 Effect of dielectric substrate

Another important concern which is placing the dielectric substrate on the FSS, for its importance in providing stability in angular response and structural support.

Adding a dielectric substrate can have an impact on the frequency response in two ways. First, depending on how we place the dielectric substrate and the thickness of the substrate, the resonance frequency will be affected and changed [1].

If the periodic structure was fully surrounded by an infinite dielectric material, the resonant frequency would reduce with the factor $\sqrt{\varepsilon_r}$, but by reducing the dielectric slab the resonance will be between f_0 and $f_0/\sqrt{\varepsilon_r}$. Otherwise, in case of placing the dielectric substrate only in one side of the periodic structure, the new frequency resonance frequency will be $f_0/\frac{\sqrt{(\varepsilon r+1)}}{2}$.

Although, FSS dielectric arrangements will influence the FSS performance over a range of incident angles. And according to Snell's law of refraction, the use of dielectric slabs might cause a less sensitivity in FSS structure [13].

2.4.3 Polarization and incident angle

When designing an FSS that operates over a wide range of incident angels, we should consider that the signals in reality arrive at various angles and have different polarization so, the propagation direction may not be controllable or known. For that reason, when designing an FSS we should guarantee that transmission and reflection properties of FSS have a stable frequency response when the angle of incidence or polarization changes.

Fundamentally, the frequency response can be affected by the polarization of the incident angle in two ways. This mainly depends on the mode of incident angle if it is TM or TE wave, Figure 2.9 shows an example of two vertical polarization scenarios. TE-wave and TM-wave incidence, where, since the electric field is in the same direction of the strips for both cases, therefore the strips will act like an inductive element.

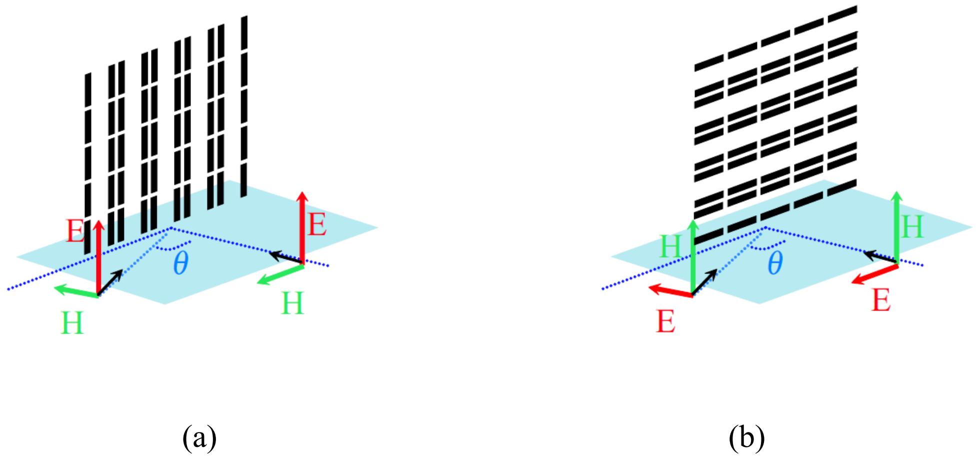

Figure 2.9 : Wave incidence on inductive conducting strips, which the square loop. (a) TE-wave incidence (b) TM-wave incidence

2.5 Analyzing Techniques of FSS

There are many methods and techniques to analysis the scattering wave from a periodic structure, such as Methods of Moments (MoM), Finite Element Method (FEM), finite-difference time-domain (FDTD), mutual impedance method, and Equivalent Circuit (EC) method.

This can usually be done by studying the response of a single unit cell of the FSS and then perform the impact of periodicity using Floquet boundary condition.

2.5.1 Methods of moment

Methods of moment is one of the earliest approaches used in evaluating the scattering from an FSS structure [14]. The MoM can handle only periodic structures supported by homogeneous dielectric substrate.

By matching the tangential field at the surface with the evaluated current on the conducting element, this will form an integral equation for the unknown currents. This results in an unknown electric field which is a function of the unknown current, which will result as a set of Floquet harmonics. These analyses can be done with the help of periodic green's function. Since MoM is not suitable for inhomogeneous structures, other approaches were developed to handle them, such as, FDTD and FEM [14,15].

2.5.2 Finite element method

FEM is one of the most used methods in analyzing FSS structures. Comparing with MoM, which known to be simple and easily applied and solved on periodic structures, FEM can handle 3d structures and inhomogeneous structures [16].

2.5.3 Finite-difference time-domain

MOM an FEM methods, analysis the periodic structure in the frequency domain, unlike the Finite Difference Time domain method, which analyses in the time domain, so the solution can cover a wide frequency range in a single simulation run. The FDTD approach is a direct solution of Maxwell's time dependent curl equations [17]. FDTD can handle 3d structures and inhomogeneous dielectric substrate.

2.5.4 Mutual impedance methods

This method was developed by Munk [1] to calculate the field scattered from the FSS. this can be done by determining the voltage induced by the incident wave at the element and also the mutual impedance between elements [18].

2.5.5 Equivalent circuit method

Equivalent circuit method is a simple method compared to the others methods which are familiar with. It provides accurate results for a simple FSS with a linear polarizations and simple element geometries at normal incidence angle. To model an FSS structure as inductive and capacitive components in a transmission line with consideration of dielectric substrates and signal incident angles [19,20]. EC performs for simple shapes, an accurate and realistic results using computer programs compared with other methods.

2.6 Grating lobes Phenomenon

Grating lobes are defined as unwanted secondary main propagation waves occurring between two neighboring elements at angles with higher order constructive interferences, when the inter-element spacing is electrically large compared to the wavelength. To prevent grating lobes from occurring, element size and spacing between elements should be kept less than one wavelength at zero-degree incidence. Figure 2.10 represents an example of how spacing between elements can result on occurring of grating lobes, where (a) shows that when the spacing between element is less than the wavelength, the radiation pattern of the radiated wave with a single main beam will occur without the presence of grating lobes. Otherwise, as illustrated in (b) the grating lobes will occur since the spacing between element is larger than the wavelength [1].

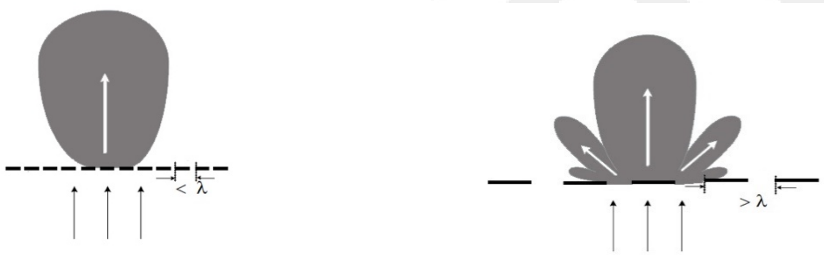

Figure 2.10 : Grating lobes occurrence in different element separation. (a) Single main beam without grating lobes. (b) Grating lobes occur when the distance is larger.

Figure 2.10 shows a grating lobes condition with inter element spacing D_x, where the angle of incidence is denoted by η, as we see a delay in each element by $\beta D_x \sin \eta$ with respect to the adjacent element. η_g represents the grating lobe direction. So, the total phase delay will be $\beta D_x (\sin \eta + \sin \eta_g)$.

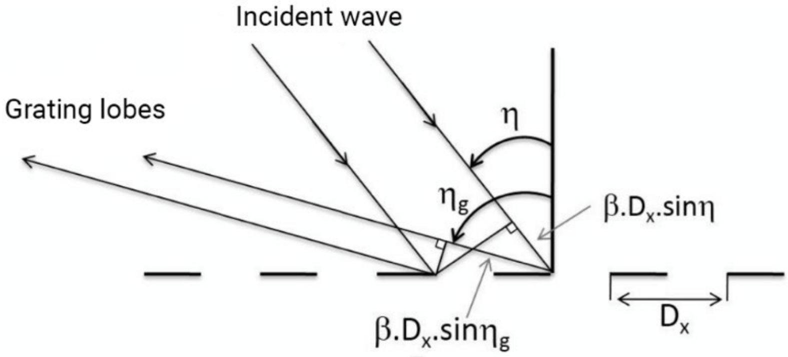

Figure 2.11 : Grating lobes phenomena [1].

This will lead to,

$$\beta D_x(\sin\eta + \sin\eta_s) = 2\pi n \tag{2.3}$$

Where,

n = 1,2, 3, …

$$\beta = \frac{2\pi}{\eta_g} \tag{2.4}$$

$$f_g = \frac{nc}{D_x\left(\sin\eta + \sin\eta_g\right)} \tag{2.5}$$

So, while designing, it is very important to be careful about element interspacing, which must be less than one wavelength to avoid grating lobes from occurrence [1].

3. ANALYSIS OF PERIODIC STRUCTURES

Analyzing and designing any microwave device requires modelling its periodic planar structures. This will require using efficient tools readily available in order to characterize its behavior. All the analysis applied to the periodic arrays are driven from Maxwell's equations. The applied tool features most be robustness, easy implementation, accurate with computational efficiency. Of course, there is no one tool that can satisfy all the mentioned characteristics. This will force the user to use a tool according to their priority in analyzing the proposed the electromagnetic problem.

There are many methods applied in analyzing periodic structures such as Methods of Moments (MoM), Finite Element Method (FEM), finite-difference time-domain (FDTD) or Transmission Line Matrix (TLM) method, mutual impedance method, and Equivalent Circuit (EC) method. However, commercial software packages such as High Frequency Structure Simulator (HFSS) based on full-wave FEM and CST Microstrips TM based on TLM method has also been utilized as modelling tools mostly to corroborate the results. This software will be used to obtain the currents excited on the elements by solving the electric field integral equation. Also, determine the corresponding reflection and transmission coefficients in each interface for each Floquet Space.

3.1 Propagation in Periodic Structure

To study the propagation in a periodic structure, first of all we have to consider the electromagnetic scattered from the periodic structure, where this can be obtained by relating the surface currents induced on the surface by the incident plane wave. The fundamental approach of analyzing any periodic structure is Floquet's theorem. Where Floquet's theorem is used in the analysis of structures that have an infinite number of periods, which is named after the French mathematician G. Floquet whose work on the periodic solution of differential equations initiated the theorem.

3.1.1 Floquet theorem

Based on Floquet's theorem, any planar periodic function can be expanded as an infinite superposition of Floquet harmonics.

Let us consider 1D periodic surface in x direction (Figure 3.1) with a period p, where u(x) is the field reacted with the periodic surface. In this case, the geometric periodicity forces the field to be periodic.

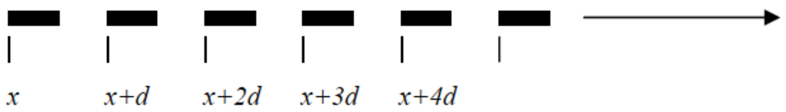

Figure 3.1 : 1D periodic structure.

If we consider the 1D periodic structure in x direction, the field reacting with periodic surface will be:

$$u(\mathrm{x+d}) = \mathrm{C}\ u(\mathrm{x}) \tag{3.1}$$

$$u(\mathrm{x+3d}) = \mathrm{C}\ u(\mathrm{x+2d}) \tag{3.3}$$

$$u(\mathrm{x+nd}) = \mathrm{C}\ u(\mathrm{x+(n\text{-}1)\ d}) \tag{3.4}$$

$$u(\mathrm{x+d}) = \mathrm{C}^{\mathrm{n}}\ u(\mathrm{x}) \tag{3.5}$$

where for boundedness $|C| \leq 1$. And we will have $C = e^{-jkd}$, k = complex constant.

then if we define a periodic function $P(x)$, where

$$P(x) = e^{-jkx}\ u(\mathrm{x}) \tag{3.6}$$

$$P(x+d) = e^{-jk(x+d)}\ u(\mathrm{x+d}) = \ e^{-jk(x+d)}\ \mathrm{C}\ u(\mathrm{x}) \tag{3.7}$$

if we substitute $C = e^{-jkd}$, we will have

$$P(x+d)= e^{-jkx}\ e^{-jkd} e^{jkd}\ u(\mathrm{x}) \tag{3.8}$$

$$= e^{-jkx}\, u(\mathrm{x}) = P(x) \tag{3.9}$$

Then,

$$P(x + nd) = P(x) \tag{3.10}$$

where P(x) has the same period as the geometry, and since P(x) is periodic in x, we can express it via Fourier series:

$$P(x) = \sum_{n=-\infty}^{\infty} P_n\, e^{j\frac{2\pi\, n}{d}x} \tag{3.11}$$

by substituting $P(x) = e^{-jkx}\, u(\mathrm{x})$,

$$e^{-jkx} u(x) = \sum_{n=-\infty}^{\infty} P_n\, e^{j\frac{2\pi\, n}{d}x} \tag{3.12}$$

$$u(x) = \sum_{n=-\infty}^{\infty} P_n\, e^{j\frac{2\pi\, n}{d}x} e^{jkx} \tag{3.13}$$

$$u(x) = \sum_{n=-\infty}^{\infty} P_n\, e^{jk_{xn}x} \tag{3.14}$$

where,

$$K_{xn} = K + \frac{2\pi n}{d} \tag{3.15}$$

This is the harmonic expansion of the field $u(x)$, and each term represents a spatial floquet harmonic infinite series and all terms propagate along the periodic axis. As we stated earlier, according to Floquet's theorem, since any planar periodic function can be expanded as an infinite superposition of Floquet harmonics, then we can easily generalize higher dimensions with more complex periodicities.

Now if we consider a TM_z polarized plane wave incident on a co-planar periodic grating of metallic strips for 1D structure (Figure 3.2).

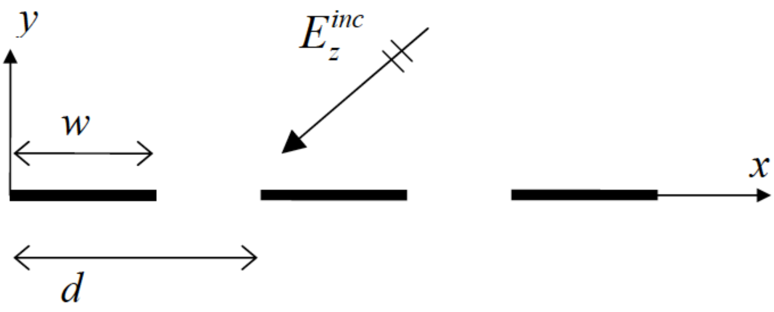

Figure 3.2 : 1D strip with TM polarized incident wave.

from (Figure 3.2) we can generalize the electric field of the incident wave striping the 1D structure,

$$E_z^{inc}(x+d,y) = e^{jk_0((x+d)\,cos^{\emptyset^{inc}}+y\,sin^{\emptyset^{inc}})} \tag{3.16}$$

$$= e^{jk_0dcos^{\emptyset^{inc}}}\quad e^{jk_0(xcos^{\emptyset^{inc}}+y\,sin^{\emptyset^{inc}})}$$

$$= E_z^{inc}\; e^{jk_0dcos^{\emptyset^{inc}}} \tag{3.17}$$

where we can define the complex constant as,

$$\mathrm{C} = e^{jk_0dcos^{\emptyset^{inc}}} \tag{3.18}$$

and

$$\mathrm{K} = K_0cos\emptyset^{inc} \tag{3.19}$$

Mainly our first aim is to compute the field scattered by the periodic strip, where the scattered field can be represented as a function of Floquet harmonics:

$$E_z^{scat}(x,y) = \sum_{n=-\infty}^{\infty} a_n(y)\; e^{jk_{xn}x} \tag{3.20}$$

and each harmonic must satisfy wave equation, where the sum of harmonics will be equal to:

$$E^{tot}(x,0)|_{nd\le x\le nd+w} = 0 \tag{3.21}$$

From the above equations we can see that the coefficients are independent of z since the source and the geometry are independent, where the coefficient of each harmonic is a function if y under the boundary condition is y = 0.

The scattered field must satisfy the wave equation where,

$$\nabla^2 E_z^{scat} + K_0^2 E_z^{scat} = 0 \tag{3.22}$$

$$\left(\frac{\partial^2}{\partial x^2} + \frac{\partial^2}{\partial y^2} + K_0^2\right) E_z^{scat} = 0 \tag{3.23}$$

Under these conditions $a_n(y)$ will be equal to,

$$a_n(y) = C_n e^{\pm jK_{yn}y} \tag{3.24}$$

where,

$$\{(-)y > 0, (+)y < 0\} \tag{3.25}$$

By substituting this into the wave equation,

$$\left(\frac{\partial^2}{\partial x^2} + \frac{\partial^2}{\partial y^2} + K_0^2\right) C_n e^{\pm jK_{yn}y}\, e^{jk_{xn}x} = 0 \tag{3.26}$$

$$(K_0^2 - K_{xn}^2 - K_{yn}^2) = 0 \tag{3.27}$$

$$K_{yn} = \sqrt{K_0^2 - K_{xn}^2} \tag{3.28}$$

Therefore,

$$E_z^{scat}(x,y) = \sum_{n=-\infty}^{\infty} C_n \, e^{jk_{xn}x} e^{-jk_{yn}|y|} \tag{3.27}$$

Where C_n represents the coefficient of complex amplitudes of each harmonic, and they will be based on the boundary conditions on the strip surface. These coefficients can be determined by many methods, one of them is the method of moments.

First of all, the angular spectrum of the Floquet Harmonic expansion is independent of the coefficients C_n, therefore

$$K_{nx} = k + \frac{2\pi n}{d} = k_0 cos^{inc\emptyset} + \frac{2\pi n}{d} \tag{3.28}$$

Therefore,

$$K_{yn} = \sqrt{K_0^2 - \left(k_0 cos^{inc\emptyset} + \frac{2\pi n}{d}\right)^2} \tag{3.29}$$

And since n varies from -∞ to +∞, then K_{nx} will also vary in the same interval, this will lead us to,

$$K_{yn} = \begin{cases} \sqrt{K_0^2 - K_{xn}^2} \\ -j\sqrt{K_0^2 - K_{xn}^2} \end{cases}, \begin{cases} K_0^2 \geq K_{xn}^2 \\ K_0^2 \leq K_{xn}^2 \end{cases} \tag{3.30}$$

If we assumed that K_0 is real, this will make K_{yn} a finite set f purely propagating modes, and an infinite set of evanescent modes.

Where, the multiple propagating modes can be scattered off the periodic surface. The angle of the propagating modes is defined as:

$$K_{xn} = K_0 \left(cos^{inc\emptyset} + \frac{n}{d}\right) \tag{3.31}$$

$$K_{yn} = K_0 \sqrt{1 - \left(cos^{inc\emptyset} + \frac{n}{d}\right)^2} \tag{3.32}$$

$$\emptyset^s = \tan^{-1}\left(\frac{K_{yn}}{K_{xn}}\right) \tag{3.33}$$

3.2 FSS Analysis with Equivalent Circuit Model

Unlike high accuracy numerical methods that require calculations using a computer, "Equivalent Circuit Model" is a simple and analytical calculation technique. It is frequently used today because they help explain the behavior of FSS. FSSs are modeled on transmission lines using equivalent circuits. Equivalent circuit model is based on the study of modeling periodic grids by Marcuvitz. It was first applied by Anderson to frequency selective surfaces [21].

Let us assume we have a periodic surface consisting of metal strips represented in Figure 3.3 with planar wave creating θ and φ angles. If the tangential components of the electric field of the wave are in the direction of metal grids as represented in Figure 3.4, the periodic structure shows an inductive characteristic that allows little transmission in low frequencies and allows transmission in high frequencies.

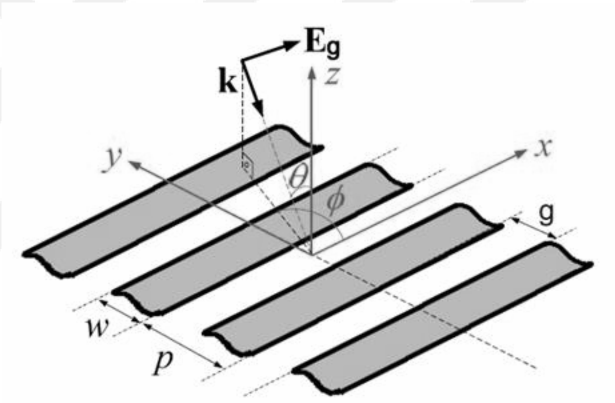

Figure 3.3 : Periodic structure consisting of parallel metal grids [50].

In the transmission line whose characteristic impedance is equal to the characteristic impedance (377 Ω) of the gap, the circuit model is drawn equivalent to a short-circuit inductive element to ground. The parameters that determine the value of the transmission coefficient (S_{21}) of the periodic structure are the width of the grids (w), the distance between them (p), the angle of polarization (φ), and the angle of incoming wave (θ).

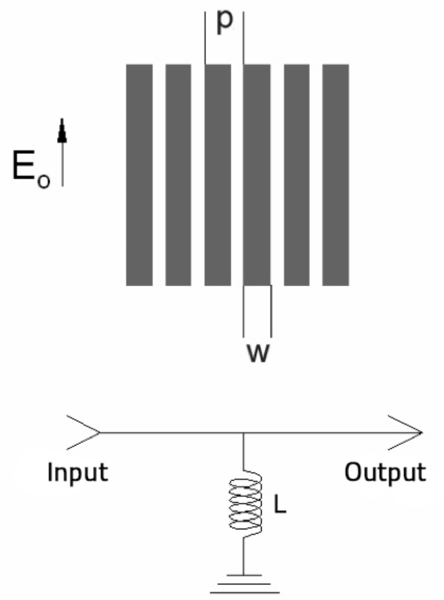

Figure 3.4 : Tangential components of the electric field in the direction of the grid [20].

If the tangential components of the electric field of the incoming wave are ninety degrees perpendicular to the metal grids shown in Figure 3.5, the periodic structure shows a capacitive response that allows transmission at low frequencies and not at high frequencies.

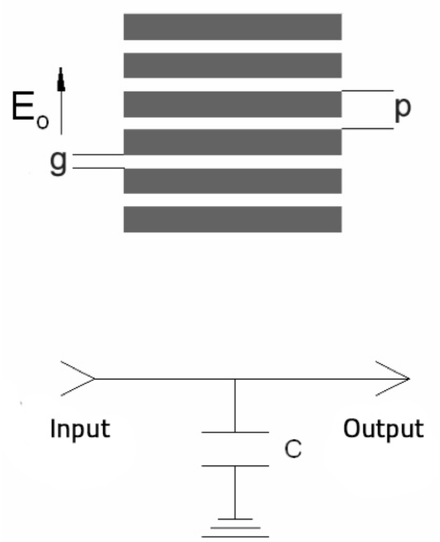

Figure 3.5 : Tangential components of the magnetic field in the direction of the grid [12].

In the transmission line which is equal to the characteristic impedance (377ohm) of the characteristic impedance gap, a circuit model equivalent to a short-circuit capacitive element is drawn to ground. The parameters that determine the value of the transmission coefficient (S_{21}) of the periodic structure are the gap between the grids (p-w), the periodic distance between them (p), the angles of the incoming wave (θ), (φ) and polarization.

Figure 3.4 represents the normalized reactance (TE polarization, $\emptyset$ = 90°) of FSS, where Figure 3.5 represents the normalized susceptibility (TM polarization, $\emptyset$ = 0°) of FSS, were these are formulated by Marcuvitz. The situation where the lengths of conductive strips (d) is finite can be defined by adding the factor "d / p" as a factor to the expressions of reactance and susceptance [19, 20].

For the case where the conductive strips are finite, TE polarization susceptibility and TM polarization reactance expressions can be completed by simplifying expressions and shown in the equations below [20, 22].

λ : Wavelength of incoming wave in free-space

g: Distance between conductors

A, G: Correction functions

Z_0: Characteristic impedance

w: Conductive strips thickness

ω: Angular frequency

$$X_{TE} = \frac{wL}{Z_0} = \frac{d}{p}.\frac{p\cos(\theta)}{\lambda}\left(-\ln\beta + \frac{A}{D}\right), \beta = \left(\frac{w}{p}\right)\left(\frac{\pi}{2}\right), \emptyset = 90^{\circ} \tag{3.34}$$

$$B_{TE} = \frac{wC}{Y_0} = \frac{d}{p}.\frac{p\sec(\theta)}{\lambda}\left(-\ln\beta + \frac{A}{D}\right), \beta = \left(\frac{g}{p}\right)\left(\frac{\pi}{2}\right), \emptyset = 0^{\circ} \tag{3.35}$$

$$X_{TM} = \frac{wL}{Z_0} = \frac{d}{p}.\frac{p\sec(\theta)}{\lambda}\left(-\ln\beta + \frac{A}{D}\right), \beta = \left(\frac{w}{p}\right)\left(\frac{\pi}{2}\right), \emptyset = 0^{\circ} \tag{3.36}$$

$$B_{TM} = \frac{wC}{Y_0} = \frac{d}{p}.\frac{p\cos(\theta)}{\lambda}\left(-\ln\beta + \frac{A}{D}\right), \beta = \left(\frac{g}{p}\right)\left(\frac{\pi}{2}\right), \emptyset = 90^{\circ} \tag{3.37}$$

$$\begin{aligned} D = {} & (1 - 0.25\beta^2)^2 + \beta^2(1 + 0.5\beta^2 - 0.125\beta^4)(A_+A_-) \\ & + 2\beta^6 A_+A_- \end{aligned} \tag{3.38}$$

$$A = 0.5(1-\beta^2)^2[(1-0.25\beta^2)(A_+A_-) + 2\beta^2 A_+A_-] \tag{3.39}$$

$$A_{\pm} = \frac{1}{\sqrt{1-\left(\frac{p\,cos\theta}{\lambda}\right)^2 \pm 2\frac{p}{\lambda}\sin\theta\sin\emptyset}} - 1 \tag{3.40}$$

In order to obtain reflection and transmission coefficients of FSS, the equivalent circuit model in Figure 3.6 is taken into consideration.

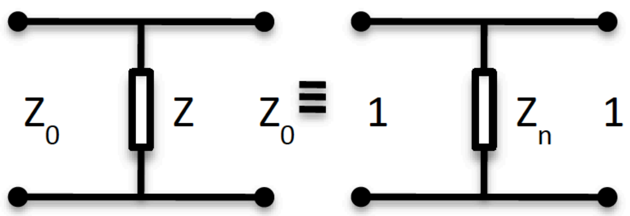

Figure 3.6 : Equivalent circuit model.

FSS is placed in the middle of the transmission line with the characteristic impedance "Z_0" and the value of its impedance is shown as "Z". The normalized impedance of FSS is shown as "$Z_n=Z/Z_0$".

In order to obtain transmission and reflection coefficients, ABCD parameters of the model were calculated in Equality below,

$$\begin{bmatrix} A & B \\ C & D \end{bmatrix} = \begin{bmatrix} 1 & 0 \\ \frac{1}{Z} & 1 \end{bmatrix} \tag{3.41}$$

Using the equation above and the relationship of the scattering matrix with the ABCD parameters, the transmission and reflection coefficients of FSS are obtained as follows.

$$\begin{bmatrix} S_{11} & S_{21} \\ S_{12} & S_{22} \end{bmatrix} = \begin{bmatrix} \frac{A+B-C-D}{A+B+C+D} & \frac{2(AD-BC)}{A+B+C+D} \\ \frac{2}{A+B+C+D} & \frac{-A+B-C+D}{A+B+C+D} \end{bmatrix}$$

$$= \begin{bmatrix} \frac{-1}{1+2Z_n} & \frac{2Z_n}{1+2Z_n} \\ \frac{2Z_n}{1+2Z_n} & \frac{-1}{1+2Z_n} \end{bmatrix} \tag{3.41}$$

$$S_{11} = \frac{-1}{1 + 2Z_n} \tag{3.42}$$

$$S_{21} = \frac{2Z_n}{1 + 2Z_n} \tag{3.43}$$

Equivalent circuit model is defined below to the frequency value calculated by Equation below, where unwanted grating lobes will show up. At higher frequencies, high-order Floquet modes start to spread and the equivalent circuit model is no longer valid.

$$f < \frac{c}{p(1 + \sin\eta)} \tag{3.44}$$

where,

η: incidence wave angle.

3.2.1 Series resonance circuits

They are modeled with patch type FSS serial RLC equivalent circuit. Figure 3.7 shows the serial RLC resonator circuit and frequency response. The circuit's input impedance (Z_{in}), resonance frequency (f_0), quality factor at resonance frequency (Q_0) and half power bandwidth (BW) at resonance frequency are calculated as shown in Equation (3.45) - (3.48). According to Equality (3.48), when the equivalent resistance or capacity of FSS increases, the bandwidth increases and when the equivalent inductance value increases, the bandwidth narrow down and decreases.

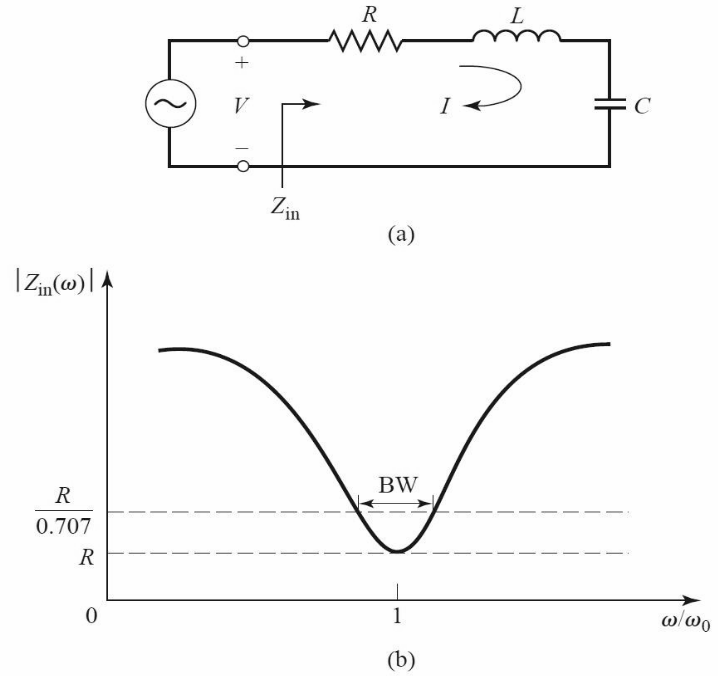

Figure 3.7 : (a) Series RLC resonator circuit (b) Frequency response.

$$Z_{in} = R + jwL - j\frac{1}{wC} \tag{3.45}$$

$$f_0 = \frac{1}{2\pi\sqrt{LC}} \tag{3.46}$$

$$Q_0 = \frac{w_0 L}{R} = \frac{1}{w_0 RC} \tag{3.47}$$

$$BW = \frac{1}{Q_0} = \frac{\Delta f}{f_0} = \frac{R}{w_0 L} = \frac{w_0 RC}{1} \tag{3.48}$$

4. STRUCTURAL HEALTH MONITORING

Structural Health Monitoring, is an area of growing interest and it is widely applied in many engineering sectors due to its importance in detecting damages and structural changes in bridges, tunnels and building over the past years [23].

These changes can refer to many factors including, change in material or geometric properties of a structure. This might happen due to many internal and external reasons such as, the age of the structure, an incorrect construction process and maybe an environmental reason. This makes Structural health monitoring essential for its importance in predicting the remaining lifetime of a structure or in the case for example if an earthquake happened SHM can be used to make quick analyses for the structures to record the magnitude of damage. Countries are spending a lot of effort, time, and money to develop Structural health monitoring.

4.1 Sensors used in Structural Health Monitoring

Over the past years, researchers and engineers were trying to develop many sensors to be applied in Structural health monitoring to monitor structures. These sensors were in the beginning classified as wired and wireless sensors. For the complex form of wire systems and since they require installments before building the structure, Engineers tried to focus on developing and improving wireless sensors since they can be applied after the construction finishes, this was also effective in cost reduction, since installing wireless sensors don’t require components as installing wire systems. Meanwhile, these wireless sensors were also divided into two main categories; Active and Passive sensors, according to their operating system. Since active sensors require active elements such as batteries which will make the system dependent on the life time of the battery, also the complex installations and the extra expenses and also network connecting problems. This will leave the passive sensors a hot topic to investigate and improve, since it enables us to eliminate the use of AC/DC power and easier installation and maintenance. Passive sensors were lately increasingly used in structural health monitoring have shown potential as structural

4.2 Mechanics of Materials

Mechanics of materials or strength of materials deals with deformation in structure and stress-induced under loading, where it studies the behavior of this structure and calculates the stresses and strains in structural members, such as beams, columns, and shafts [24]. One of the most important parameters to be care about is the structure element geometry and its properties, they must be considered where length, depth, width, and abrupt changes can have different meanings.

Any material can be exposed to some changes due to many factors; these factors can be categorized mainly into normal strain, shear strain, column buckling, and delamination.

Unlike normal strain who shows a deformation on axial length of the object, shear strain force will be parallel to the surface of the object. This will result in a change in the angle of the object between two-line segments. If we study an object before it gets exposed to a force and hypothetically draw two orthogonal lines, since these lines are orthogonal the angle between them is $\frac{\pi}{2}$, and if we are talking about change in angle, this object when it is going to be exposed to a force a change in angle will occur.

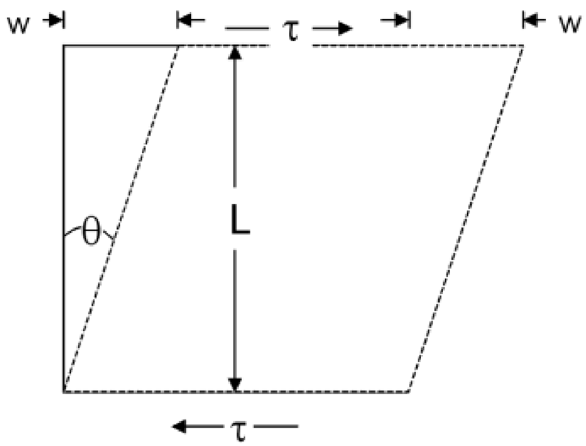

Figure 4.1 : Representation of shear strain deformation [25].

Another type of deformation is column buckling, this type of deformation usually is not related to the strength of the material, it happens due to geometric instability of the system, this means that it is not dependent on the material strength. So, Buckling can also be described as bending or bowing of a column due to a compressive load [26].

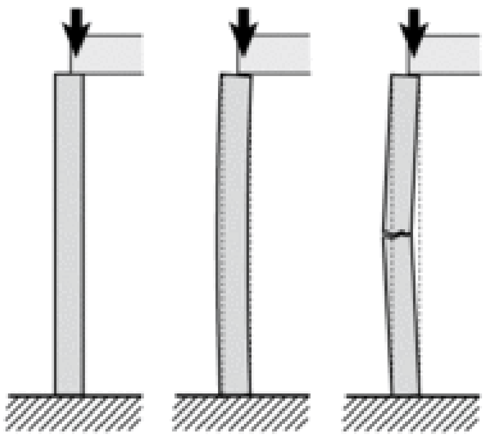

Figure 4.2 : Representation of Column buckling.

One of the most crucial damage for impacted composite is delamination. This will cause a separation between layers. Delamination is caused by matrix cracking, bending cracks, and shear cracks. It also affects the compression strength of composite laminate, and it will slowly cause the composite to experience failure through buckling [27].

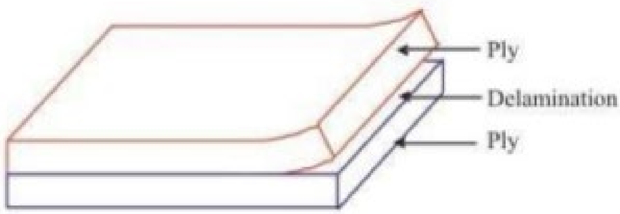

Figure 4.3 : Representation of Delamination.

5. EFFECT OF FSS GEOMETRY ON SENSING

The frequency response of any FSS structure depends on its geometry. Since we are going to use FSS as a passive sensor, it can be either embedded or mounted on surfaces. So, when any deformation occurs to the mechanics of the materials which we mounted FSS on it will result in deformation as well in the FSS structure itself. This will lead definitely to a distinguishable change in the frequency of the unit cell structure caused by the deformation.

5.1 Structural Health Monitoring Using FSS as A Passive Sensor

Structural health monitoring is a system used in structures such as, bridges, building and highways to improve the capacity of damage detection. As mentioned earlier FSS is recently used in many application fields, one of the newest potential use of it is using FSS as a passive sensor. FSS found its place in structural health monitoring, for its ability to work as a passive sensor, this is a potential area of study for its necessity over using active sensors. A main advantage of using FSS as a sensor in structural health monitoring for their high sensitivity for physical and environmental changes, this will make them an ideal basis for sensor development [28, 29]. Since FSS frequency response depend on its geometry, so any deformation will alter its frequency response.

5.2 Effect of incident angle on Normal and Curvature Surfaces

Incident angle is considered to be very critical factor while designing any FSS structure for two main reasons, one of them is the propagation direction can’t be controlled in real applications, the other one is designers try to design an FSS that can cover and operate at a wide range of incident angles. Meanwhile, frequency response of all most all the basic FSS elements design can be considered having similar frequency response to incident angles. To be more specific, incident angles can be excited in two modes of incident TE (Transverse electric) or TM (Transverse magnetic) wave. As known from electromagnetic theory, any incident angle contains E-filed components and H-field components with a certain direction. Usually, in TM mode electric field is normal to the FSS structure, while the magnetic field is parallel to it [30]. Unlike, in TE mode, electric field is parallel to the FSS structure, while the magnetic field is normal to it. In some cases, incident angle might contain same electric and magnetic components. This will result in a combination of TE and TM at the same time [4]. Usually, while designing any FSS there are some forethoughts that should be considered to alleviate the effect of incident angle on the frequency response of an FSS.

One of them, is the element spacing should be reduced as much as possible with considering the wavelength. This affectively will result on reducing the effect of phase difference between elements. The other thing is using dielectric substrate to support the FSS structure, this might be effective more in TE incidence compared with TM incidence.

These forethoughts are all for straight normal surfaces, but of course real-world structures are not like that, curved structures will have totally different response to incident angle and hence different FSS design.

Another consideration while designing an FSS structure, is that there might be a conductive ground plane or additional FSS layers. Where in the presence of ground plane on an FSS structure, FSS will act as an absorber and no transmission will occur. This is mainly because FSS will act as high impedance surface, and resonance frequency need to be controlled [35].

5.3 Effect of Deformation Situations on FSS Response

As we mentioned earlier, materials can be exposed to many different changes due to many factors, depending on the mechanics of the materials changes, FSS geometry design and frequency response will respond differently to each deformation. For that reason, FSS response for each material deformation will be studied separately.

5.3.1 Effect of normal strain on FSS response

Normal strain detection was the first deformation to be studied using metamaterials as sensor in structural health monitoring [31, 32, 33, 34]. As discussed before, Normal strain is a type of material deformation that arises as compressing or extension of a material along its axial when its exposed to a force.

As shown in Figure 5.1, normal strain, is the deformation of an object which is exposed to a force, this will result in axial changing in the length of the object. Normal strain can be represented as $\varepsilon = \delta/L$, where δ refers to the change occurred to the object after it was been exposed to a force from the end, and L represents the original length of the object. This formula can be useful to calculate for us how much the object extended or suppressed compared to its original length.

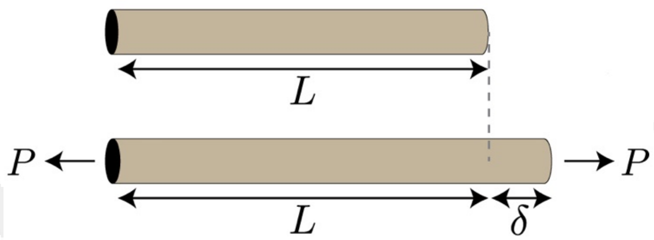

Figure 5.1 : Representation of normal strain deformation [35].

So, it has a magnitude and a direction where the magnitude is described as the extended/ compressed length (δ) over its original length (L) this can be calculated using the formula below

$$\varepsilon = \frac{\delta}{L} \tag{5.1}$$

A useful parameter when considering normal strain deformation is gauge factor, this factor helps in determining the sensitivity of FSS to normal strain. Definitely, each and every FSS geometry type will have its own gauge factor and it is calculated using [40]:

$$GF = \frac{\Delta f}{f_0 \varepsilon} \tag{5.2}$$

Where Δf is the change of resonant frequency under a normal strain modification ε. And f_0 is the original frequency response of an FSS before it's exposed to deformation [47].

5.3.2 Effect of shear strain on FSS response

Shear strain is a type of material deformation caused by rotational force(Figure 4.2) [36]. This means that the structure will be exposed to angle change, where in shear strain situation we don't have a directional vector [38]. For shear strain deformation, if we consider co-polarization and cross polarization. Where in co-polarization condition, if the signal was vertically polarized, the co-polarized is vertical polarized also. Unlike in the cross-polarization mode, where the direction is orthogonal to the desired direction, so if we send a vertically polarized signal, the cross-polarization is horizontal polarized [39]. Due to a geometrical change in the FSS structure caused by shear strain deformation, it can be noticed that shear strain has a slight effect on FSS resonance for both cross and co-polarization. This can be considered effective and an advantage for separating deformation responses between normal and shear strain. Since in this case, shear strain will not affect the co-polarization resonance frequency, from there we can understand that any shifts in resonant frequency can be considered as normal strain deformation. Cross-polarization works better with shear stain, and when shear strain increases, cross-polarization radiation will also increase. This is mainly because of easing the symmetricity of the FSS. Symmetric easing will make changes in currents generation where because of this deformation these currents will move freely. Meanwhile, adding a ground may be considered advantageous resulting in a stronger cross-polarization response compared with ungrounded FSS designs.

5.3.3 Effect of column buckling on FSS response

Designing an FSS structure for column buckling deformation might be different from other deformations. Columns in their shape has a curved structure, where in this case a straight forward FSS can't be mounted on the column. For that reason, the effects of conforming the FSS to the column's curvature should be considered. Also, columns of most structures are formed using concrete, which is a material composed of fine and coarse aggregate materials. The formation of the concrete will cause a power loss due to the existence of water inside it. This will result also in an unexpected scattering of the incident angle, which is on the other hand will cause a reduction in the power reflected form the FSS structure, as a result the resonance of the FSS structure will be hard to detect as well [28]. For this reason, designing an FSS structure in S-band might be a good option, since less dielectric loss can be conducted in lower frequencies.

Column buckling can be studied in two ways; horizontal displacement test and torsion test (Figure 4.3). The horizontal displacement will cause the steel-tube core of the column to be exposed to a vertical normal strain, which will result in a mechanical failure of the column and cause a buckling in it, where buckling usually happens near to the bottom of the steel-tube core [40].

5.3.4 Effect of delamination on FSS response

Delamination of a material is a very critical deformation form because it creates an air gap in the material and causes a failure in the structure. Many methods are applied to detect delamination in the materials, such as ultrasonic reflection tomography [42], microwave thermography [41] and due to the recent researches FSS structures can be also implemented and used to sense delamination in materials for its sensitivity to dielectric materials. For the case of delamination, using dielectric substrate might be a good option to sense this type of deformation. The resonance frequency will be changed because the FSS capacitance will be reduced, where when the distance between the substrates of delamination increases the capacitance between them accordingly will decrease. In this type of deformation, the inductance will not be altered, unlike the capacitance and the depth if the resonance frequency which will be changed due to reflection caused by the additional dielectrics. This can be considered as an advantage that can help us distinguish between other types of deformations such as shear strain, where in shear strain deformation we do not exhibit a change in the depth of resonance frequency. On the other hand, distinguishing between normal strain and delamination can be hard using this method. Another concern, is that a single FSS structure can't handle large dielectric structure, this will push us to use multiple FSS layers. Of course, the spacing between the layers must be far enough to avoid interference between FSS's resonances, since every FSS will have a different resonance frequency accordingly. For that reason, distance between layers must be not that close to avoid electric coupling between them, and at the same time not that far to avoid leaving blind spots where no delamination in this area will be detected.

6. FABRICATION OF FSS

FSSs which are created by periodic element units, are usually printed on dielectric substrates.

These substrates affect and change the frequency characteristics according to their electrical properties and their thickness. It is desired that the electrical properties of the dielectric layers are constant and their ambient temperature is not so high. Of course, there are other important considerations such as cost and the ease of getting the end product. Printing techniques vary and change according to the dielectric layer used. One of the economical and well performance dielectric layer is FR4, where FR4 stands for the flame retardant and 4 stands for woven glass reinforced epoxy resin. It is used in the manufacture of electronic printed circuit boards coated with copper on it. The properties of FR4 may depend on the manufacturer; however, it generally has favorable strength and water resistance attributes and its relative dielectric constant varies depending on the manufacturer and model also, where it is close to 4.4. In this way, firms industrial FSSs are printed on copper-coated FR4 dielectric layer. FSS surfaces can be printed on 125μm thick film layers using silkscreen printing technique and silver-based conductive materials.

7. GENERAL ANALYSIS FOR LOOP BASED FSS ELEMENTS

7.1 Loop Elements

These types of elements are formed from loops of conductors such as; circular rings, square loops, hexagonal loops and many more shapes as shown in Figure 7.1. For example, the square loop can only be spaced closely in the case of square-grid arrangement, unlike the circular. Where this consideration in addition also to the conductor width, has a main role in affecting the bandwidth and sensitivity to angle of incidence. At the same time, the resonant frequency of the FSS can be determined from the circumference of the loop. Where FSS loop elements resonates when the circumference of the loop is approximately equivalent to the operating wavelength [19]. Therefore, the desired frequency response can be determined with the use of, the conductor width, element spacing, orientation, and circumference.

Figure 7.1 : Example of loop elements.

The performance of the loop elements was studied analytical equations as well as HFSS for simulating the shapes. The main advantage of loop elements is their ability to give high performance in higher frequency resonance FSS structures. In this thesis, many FSS geometries performances were studied to disclose the best FSS geometry according to their freuqncy response to structural deformation. These geometries were all optimizied to work in the S-band frequency, where S-band varies from (2-4 GHz).

we optimize our geometries using the parametric option of the HFSS software by giving the length different values and then choosing the best value which suits our application.

If we consider the square loop element, where the square loop is optimized to have parameters of d = 30 mm, s = 10 mm, g = 1 mm, and p = 31 mm, where the mentioned parameters are shown in Figure 7.2 (a).

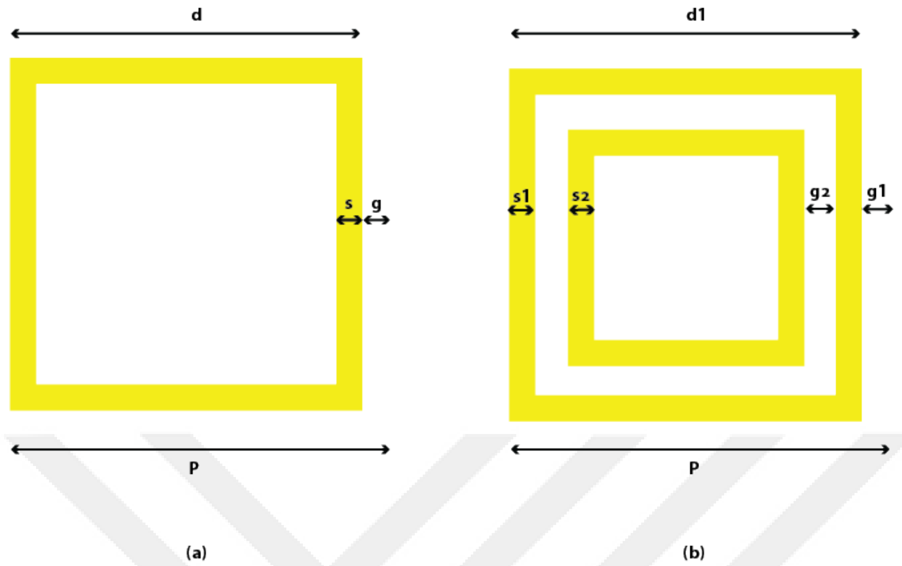

Figure 7.2 : (a) Square loop & (b) double Square loop.

Generally, loop elements have a good performance to incidence angle changing, which is a big advantage for them in most applications where stability is essential. In our case, changing the incidence angle must give us some clues to understand that some deformations have occurred to our system. The frequency response of the square loop FSS including the changes in incident angle, where these changes, are one of the most important characteristics to consider while designing an FSS passive sensor for SHM. Four values of angles are simulated from (0º to 60º) for both TE and TM. The square-loop FSS parameters design mentioned before are simulated in Figure 7.3.

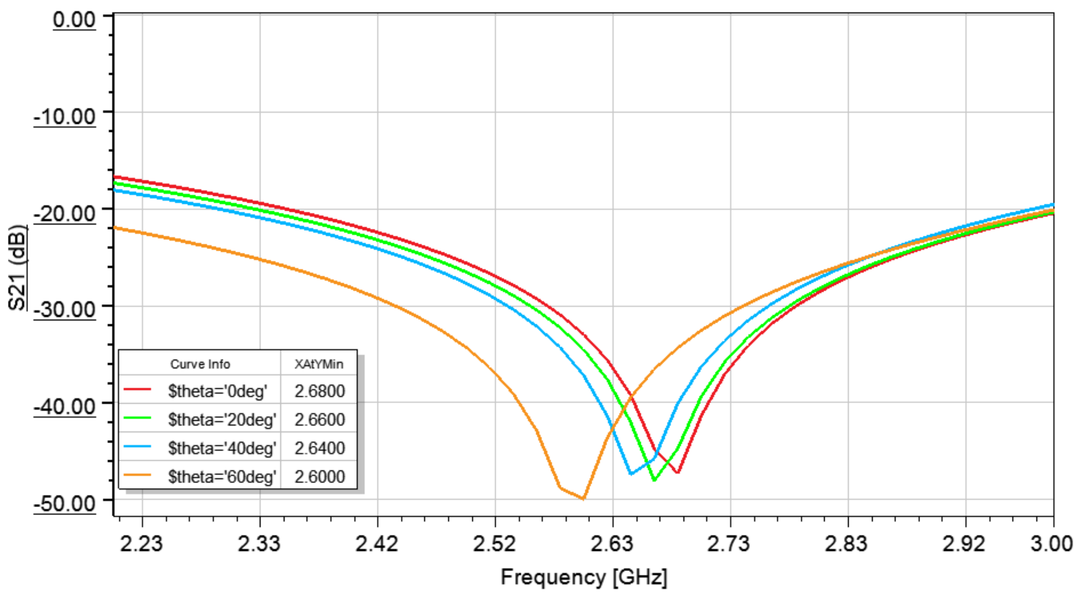

Figure 7.3 : Square loop S_{21} results for different incidence angle from 0º to 60º TE mode.

Form this simulation result we can see that the frequency response of square loop elements for different incidence angles is stable from (20º to 60º), where this as we mentioned earlier is not helpful in the case of structural health monitoring, where detecting the change in incidence angle is essential. This is clarified more in Table 7.1, where the deviation from the center frequency is not linearly increasing, and the frequency from (20º to 60º) angles is sort of stable, whereas mentioned earlier this is not good for our case since the distinction between different incidence angle frequency response is required to detect deformation occurred in structures.

Table 7.1 : Resonance frequencies of the square loop FSS with different angles in TE mode**.**

Degree (º)	Frequency (GHz)	Deviation (%)
0	2.680	0
20	2.660	0.746
40	2.640	1.492
60	2.600	2.985

Double square loop is examined and simulated as shown in Figure 7.2 (b), where the parameters studied are d1 = 30 mm, s1 = 10 mm, g = 1 mm, p = 31 mm, d2 = 20, s2 = 4mm, and g2 = 4mm.

With these parameters a better performance in detecting if a deformation occurs with changing the incident angle can be adapted, since the change is linearly increasing with the double square loop FSS, this is shown in Figure 7.4.

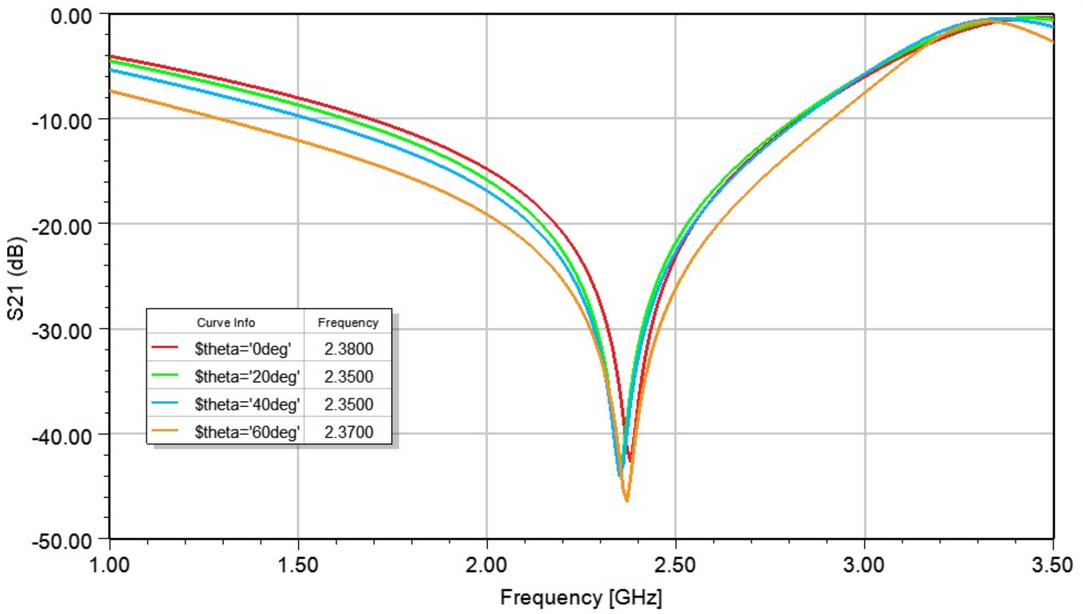

Figure 7.4 : Double square loop S_{21} results for different incidence angle from 0º to 60º TE mode.

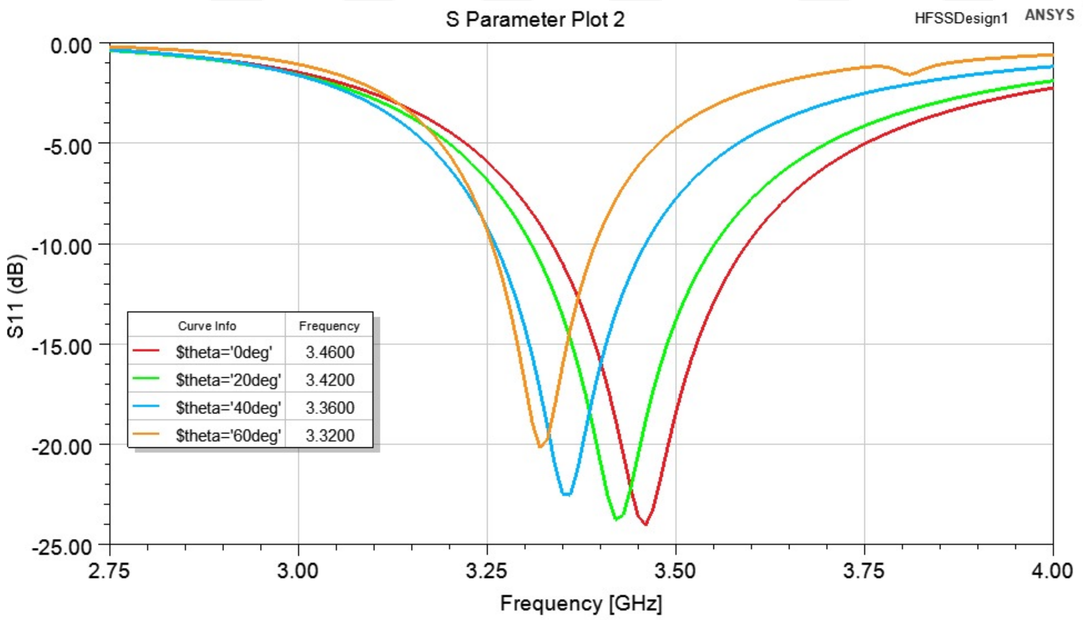

Figure 7.5 : Double square loop S_{11} results for different incidence angle from 0º to 60º TE mode.

The capacitance of the inner loop is affected by the outer loop, but at the same time the capacitance of the outer one is reduced compared with the single circle design. Although, the outer loop reactance is affected by the additional inductance created by the inner loop conductor. Table 7.2 shows a better linearly increasing deviation in the frequency response with respect to change occur in the incidence angle in TE S_{11} mode.

Table 7.2 : Resonance frequencies of the double square loop FSS with different angles in TE mode.

Degree (º)	Frequency (GHz)	Deviation (%)
0	3.460	0
20	3.420	1.156
40	3.360	2.890
60	3.320	4.046

The resonant frequency of the circular ring FSS geometry is determined by the circumference of the loop. Therefore, by determining the circumference, the width of the conductor, the space between elements, our frequency response can be determined.

The circle loop has parameters of d = 48 mm, d2 = 6 mm, g = 6 mm, and the circumference of the loop is 18 mm, where the mentioned parameters are shown in Figure 7.6 (a). Simulation results are shown in Figure 7.7 and Figure 7.8.

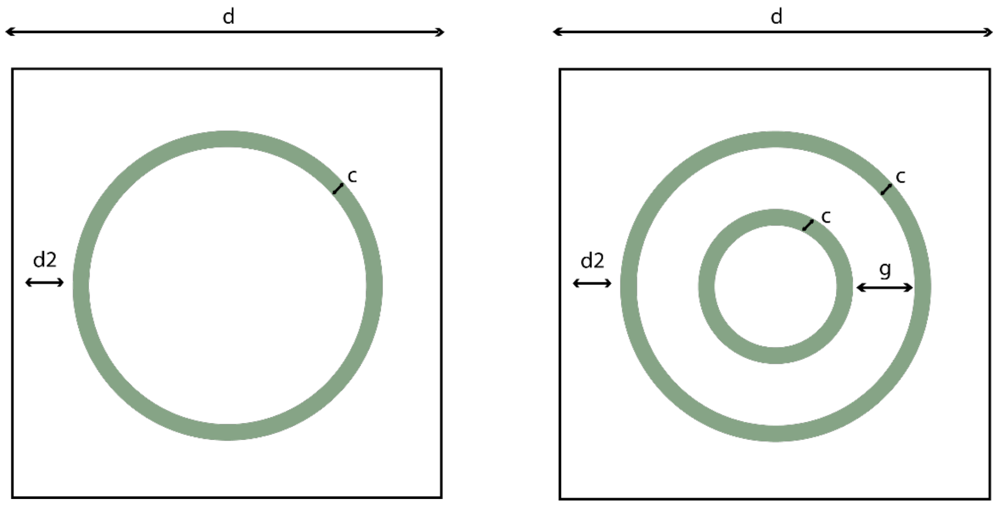

(a) (b)

Figure 7.6 : (a) Circle loop & (b) Double circle loop.

Figure 7.7 shows the frequency response in TE mode for single circle loop, we can see that it is hard to measure the reflected signal.

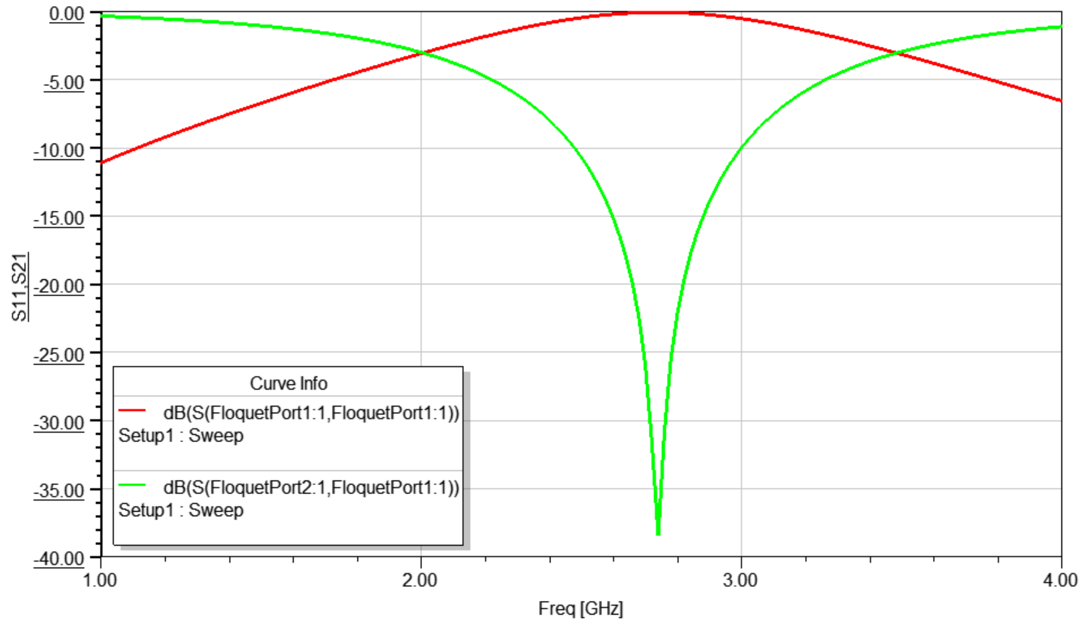

Figure 7.7 : Frequency response of circle loop in TE mode.

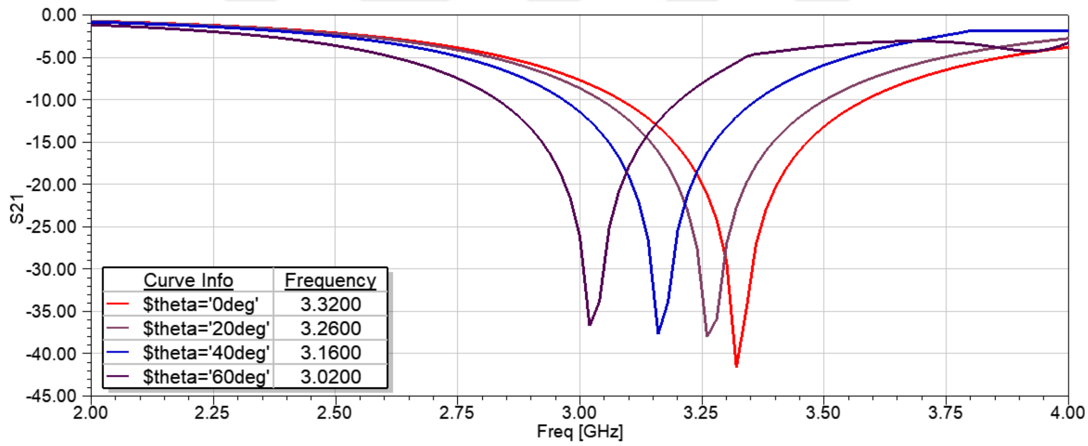

Figure 7.8 : Single circle loop S_{21} results for different incidence angle from 0º to 60º TE mode.

Form this simulation result we can see that the frequency response for a single circle loop element for different incidence angles is linearly changing, where this as we mentioned earlier is helpful in the case of structural health monitoring, where detecting the change in incidence angle is essential. This is clarified more in Table 7.3, where the deviation from the center frequency is linearly increasing,

Table 7.3 : Resonance frequencies of the circle loop FSS with different angles in TE mode.

Degree (º)	Frequency (GHz)	Deviation (%)
0	3.320	0
20	3.260	1.80
40	3.160	4.81
60	3.020	9.03

These results are quite satisfying for measuring S_{21} parameter where measuring the transmitted factor in FSS application is a familiar thing. But since we are using our FSS design as a passive sensor to mount it on any structure, it is more practical to measure reflection coefficient than transmission coefficient, since the transmitted signal will travel through the structure a lot of losses will occur and the received transmitted signal might be too weak, unlike while measuring the reflected signal no losses will be occurred.

Double circle loop as shown in Figure 7.6 (b) is examined and simulated, where the parameters studied are d = 48 mm, d2 = 6 mm, g = 6 mm, and the circumference of the outer loop is 18 mm, and g2 = 10mm and the circumference of the inner loop is 10 mm. . Figure 7.9 shows the frequency response in TE mode, as we can see, after adding the inner loop a second S_{21} resonance is created, and now between these two resonances, the reflected S_{11} resonance now is measurable.

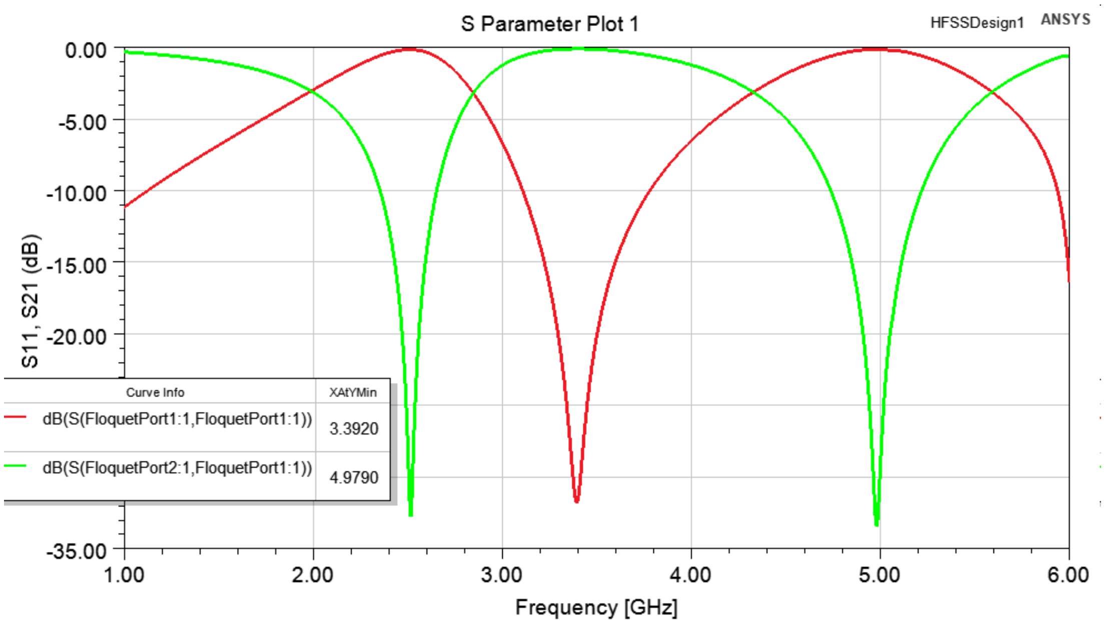

Figure 7.9 : Frequency response of double circle loop in TE mode.

With these parameters a better performance in detecting if a deformation occurs with changing the incident angle in a narrower incident angle change, where now the incident angle will be measured for each 5 degree. Measuring the change in practice is more realistic since we are measuring tilting in structures. , As shown in Figure 7.10. the frequency response is changing linearly in the reflected mode.

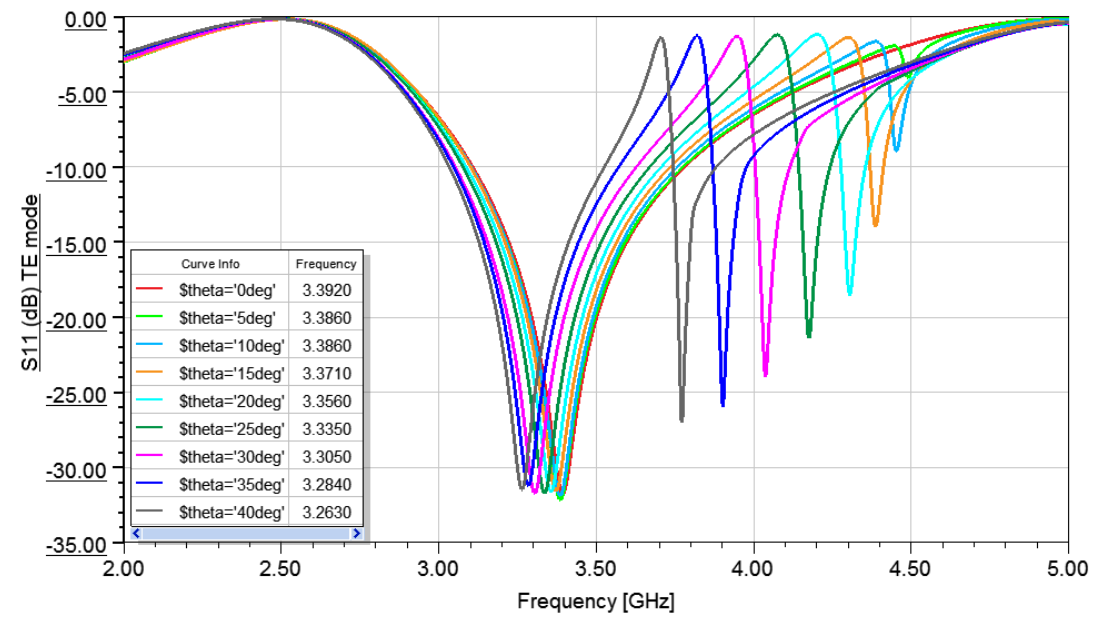

Figure 7.10 : Double circle loop S_{11} results for different incidence angle from 0º to 40º TE mode.

From this simulation result we can see that in the case of double circle FSS, the reflected signal is measurable, but at the same time, the frequency response at different angles is not changing linearly as seen in Figure 7.11.

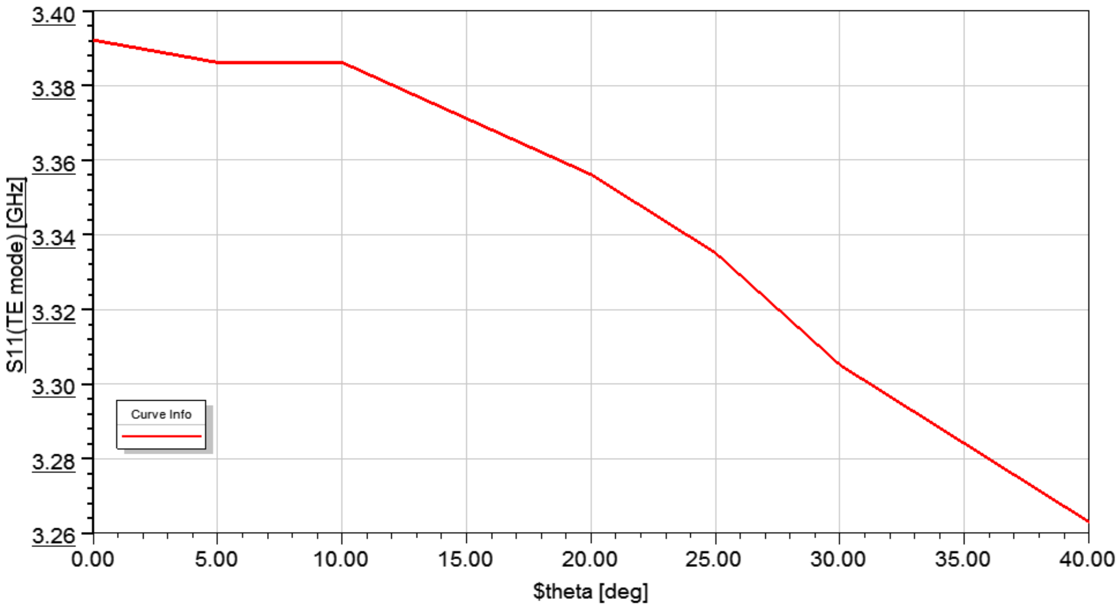

Figure 7.11 : Frequency response of double circle loop in TE mode at different angles.

8. DESIGN AND SIMULATION

8.1 Design of FSS as a Passive Sensor Based on Double Circle Element for Incident Angle Detection

Our aim of this project is to detect tilting in civil structures, where the response of the FSS while changing the incident angle should be linear for us to understand at what angle our structure is deviated.

Some FSS designs are considered to have an unstable frequency response for incident angle changing, but this is not enough for us. Our aim is to have an unstable frequency response while the structure is deviated in a linear manner.

Circular loop elements are miniaturized small elements and they have a good and stable frequency response if it is compared to dipole element for example, but at the same time if we considered the dipole elements, they will be very large in size and a large array would be a disadvantage in our case, where instead of mounting our FSS on a small area of the structure we would have to cover a larger area if we used large elements. This is not a practical solution; therefore, circular elements are more suitable.

Also, since we are not only considering sensitivity to incident angle and we want the change of the frequency response to be linear, where linearity is a very critical factor for our case.

So, for example tripole/dipole/cross dipole elements might have a better sensitivity to incident angle change, but will not give a linear performance as the bended (circular) elements will do.

The reason of using double ring loop FSS design, is that both the inner and outer loop inductance operates the same way the single circle loop operates.

The other important thing is that the inner loop creates a second S_{21}, therefore it creates a narrow S_{11} between the two resonances. Also, the distance between two neighboring inner loop geometries becomes quite large. For this reason, the angle stability of the second S_{21} resonance is quite low. This situation causes low angle stability of S_{11} resonance, where this is the goal we are looking for. Also, since circular geometries are used in the design, sudden deviations in the resonance frequency do not occur. The distance between the unit cell geometries are arranged to be large to ensure that we notice the change in structures with small angles. Although, when we increase the distance between elements, the capacity value between them decreases. In this case, the equivalent inductance value formed by the conductive paths determines the resonance. Therefore, the main reason of choosing circular loop is that frequency response changes linearly.

A modified double circle loop with a symmetrical dipole added a rounded the outer circle(Figure 8.1), this increase the capacity between the elements and this will lead the energy stored between elements to change, thus the frequency response will also be expected to change linearly, where the parameters studied are d = 50 mm, L=32 mm, d2 = 6 mm, g = 10 mm, c=2 mm, and the circumference of the outer loop is 18 mm and the circumference of the inner loop is 9 mm, and the dipole length=32 mm with 1.4 mm width.

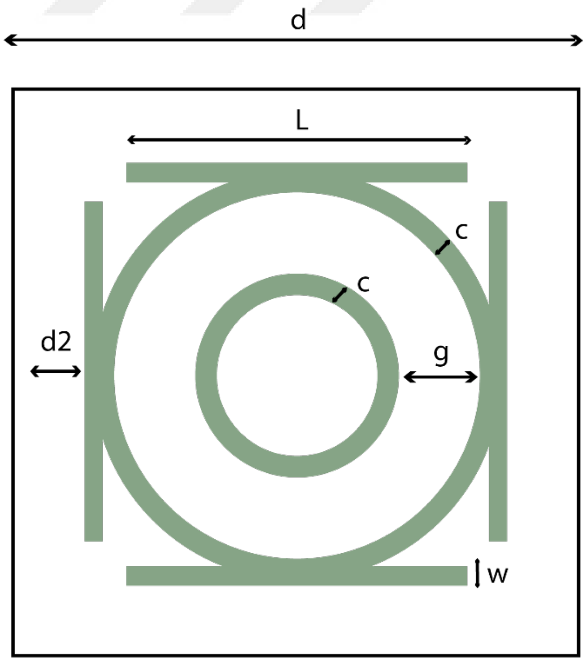

Figure 8.1 : Double circle loop with symmetrical dipoles.

As shown in Figure 8.2, Figure 8.3 and Figure 8.4 the frequency response is measured from 0 to 20 degree at five degree angle in both TE an TM mode, and the frequency response in both transmission modes is changing linearly.

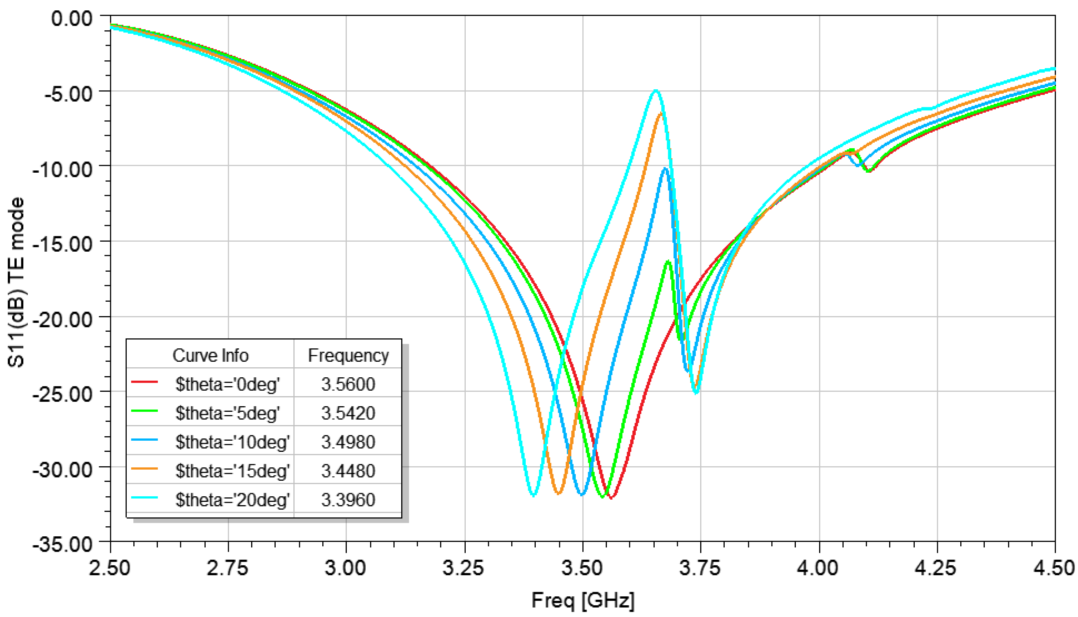

Figure 8.2 : Symmetrical double circle loop S_{11} results for different incidence angle from 0º to 20º TE mode.

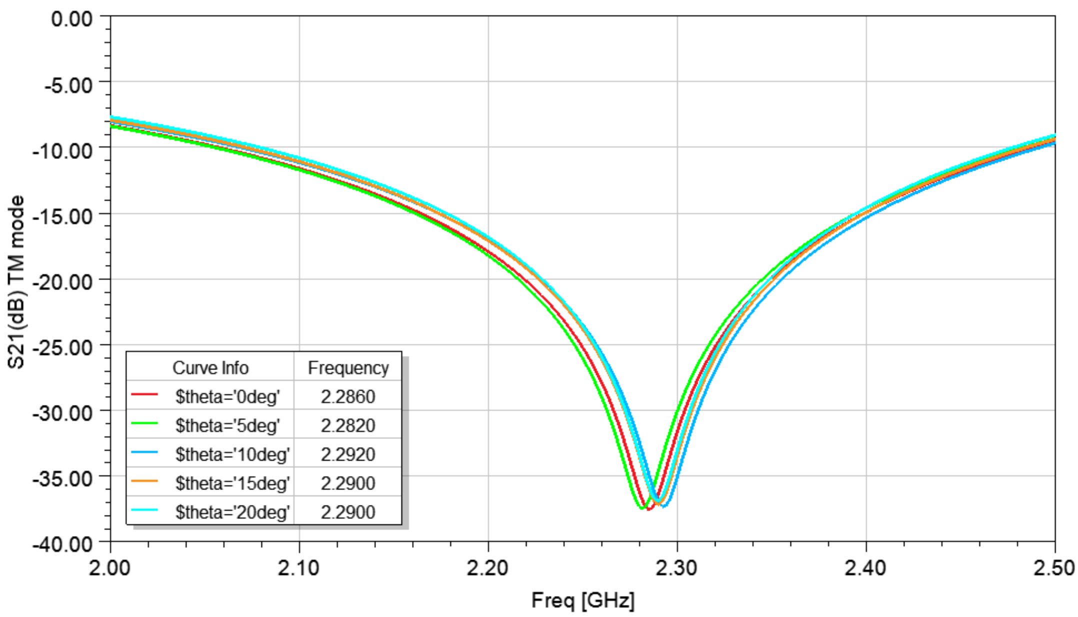

Figure 8.3 : Symmetrical double circle loop S_{21} results for different incidence angle from 0º to 20º TM mode.

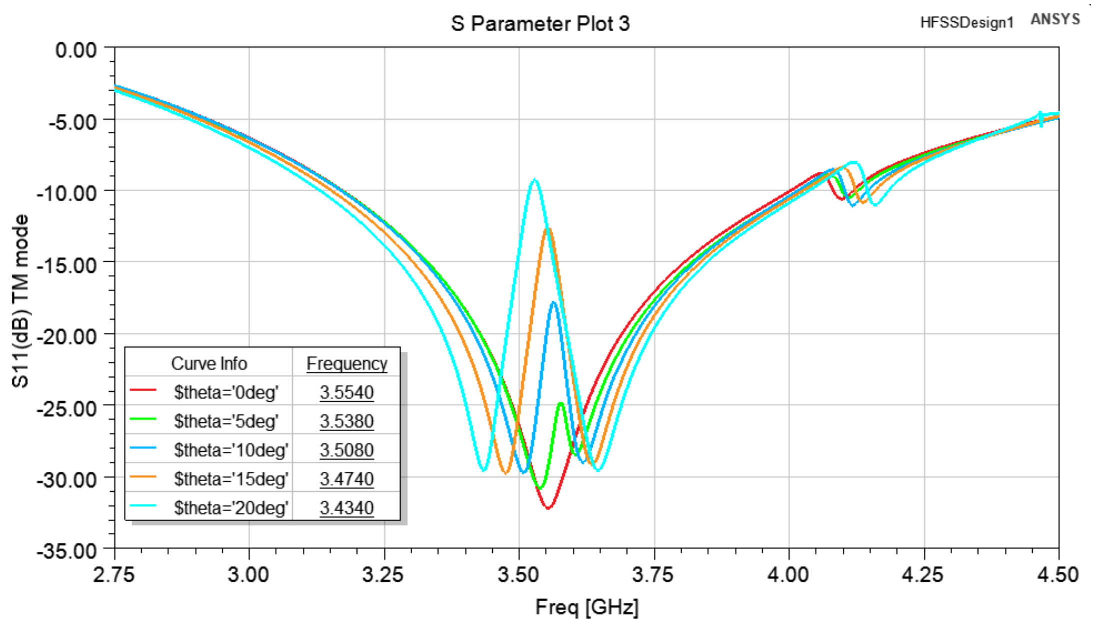

Figure 8.4 : Symmetrical double circle loop S_{11} results for different incidence angle from 0º to 20º TM mode.

But as we can see the second resonance created is affecting the main resonance in TM mode more than TE mode. Therefore, for our symmetrical design TE mode gives a better performance that TM does, for that reason the deviation factor will be calculated according to TE mode S_{11} simulations.

Table 8.1 : Resonance frequencies of the double circle loop with symmetrical dipoles with different angles in TE mode.

Degree (º)	Frequency (GHz)	Deviation (%)
0	3.560	0
5	3.542	0.505
10	3.498	1.741
15	3.448	3.146
20	3.396	4.606

From our simulations results in Table 8.1, we can notice that the deviation factor has a better performance compared to the double circle loop. From our results, we can see that our proposed design is working sufficiently well and the incident angle is changing linearly, but for a better performance and a more accurate observations, our FSS design is modified with some changes that a better deviation factor can be observed. Also, to reduce the second frequency effect on the first one. Figure 8.5 shows the final modifications of our double loop circle, where now it has an asymmetrical shape and the parameters studied are d = 50 mm, L=32 mm, d2 = 6 mm, g = 10 mm, c=2 mm, and the circumference of the outer loop is 18 mm and the circumference of the inner loop is 9 mm, and the dipole length=32 mm with 1.4 mm width.

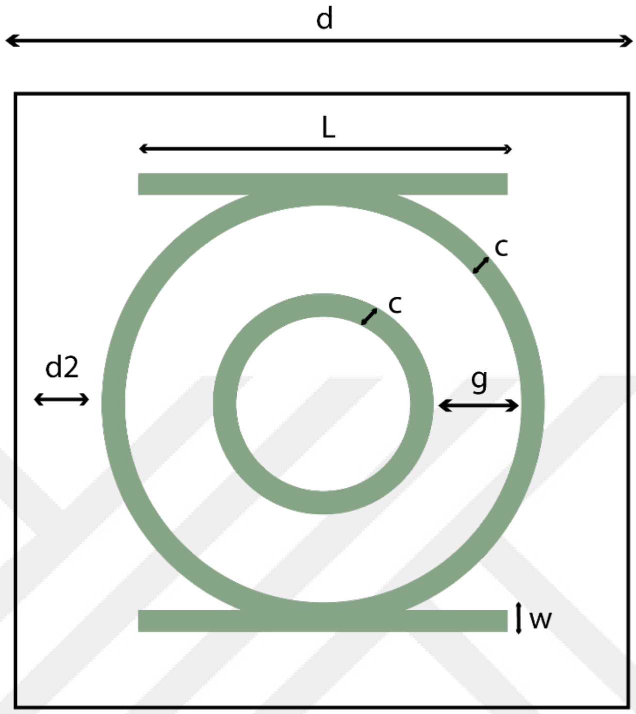

Figure 8.5 : Asymmetrical double circle loop.

By doing so, this will add a capacitive effect from the upper and lower part of the element and at the same time will increase the distance from right and left. Figure 8.6 represnets the circuit equivalent of the designed asymmetrical double circle loop shown in Figure 8.5, where the mutual inductance is the coupling effect between two FSS layers.

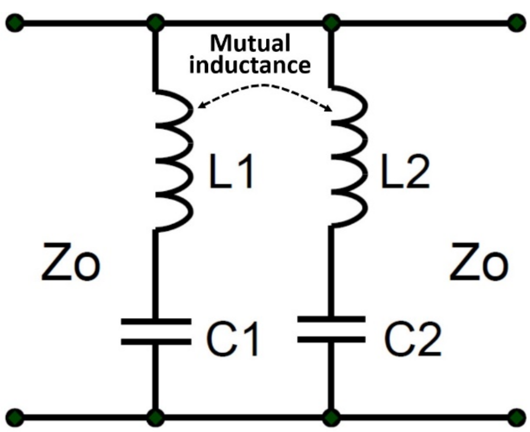

Figure 8.6 : Circuit equivalent for asymmetrical double circle loop.

Equivalent impedance of the FSS can be derived from the circuit model given in Figure 8.6 as,

$$Z = Y_1 + Y_2 \tag{8.1}$$

$$Z = \left(JwC_1 + \frac{1}{jwL_1}\right) + \left(JwC_2 + \frac{1}{jwL_2}\right) \tag{8.2}$$

$$Z = \frac{(1 - w^2 L_1 C_1)(1 - w^2 L_2 C_2)}{\mathrm{jw}(C_1 + C_2 - w^2 C_1 C_2 (L_1 + L_2))} \tag{8.3}$$

Where when the impedance Z approaches zero the frequency response will be reflected, while when Z approaches infinity the frequency response will be transmitted.

From our modified design, Figure 8.7 and Figure 8.8 represents the frequency response in TE mode, while Figure 8.9 represents the frequency response in TM mode, we can see that our FSS response in TM mode (Figure 8.9) has a better performance, since the frequency response is changing linearly and at the same time the second resonance is not close to the first resonance as it is in TE mode (Figure 8.7).

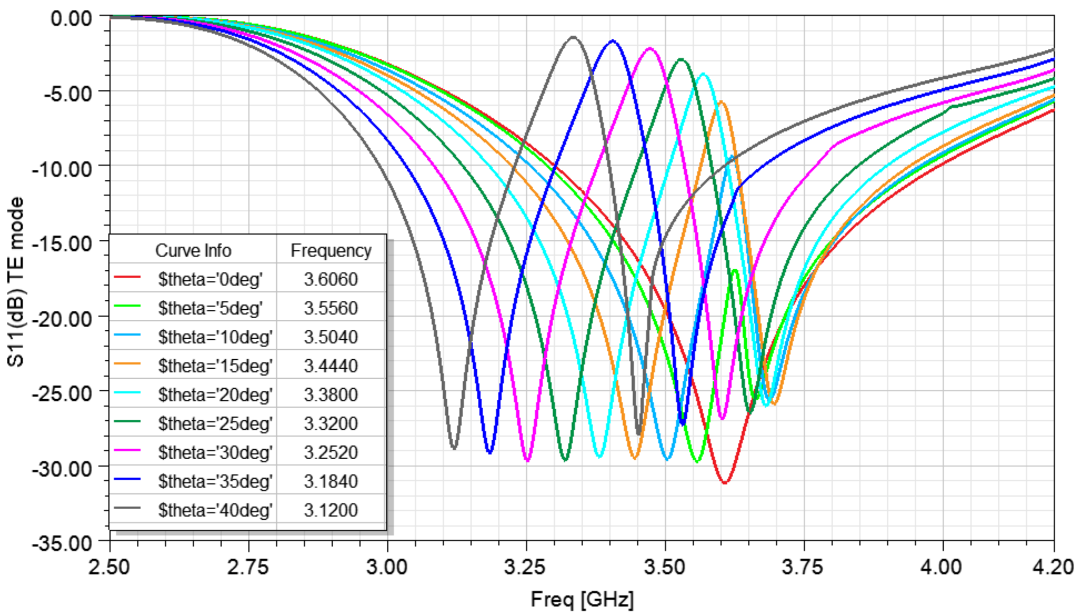

Figure 8.7 : Asymmetrical double circle loop S_{11} results for different incidence angle from 0º to 40º TE mode.

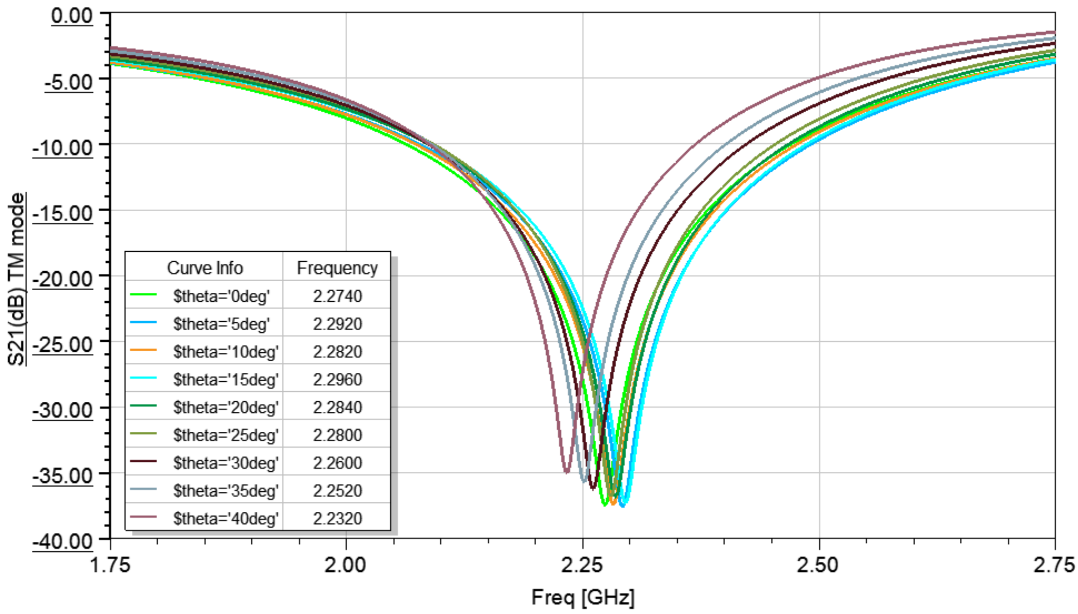

Figure 8.8 : Asymmetrical double circle loop S_{21} results for different incidence angle from 0º to 40º TM mode.

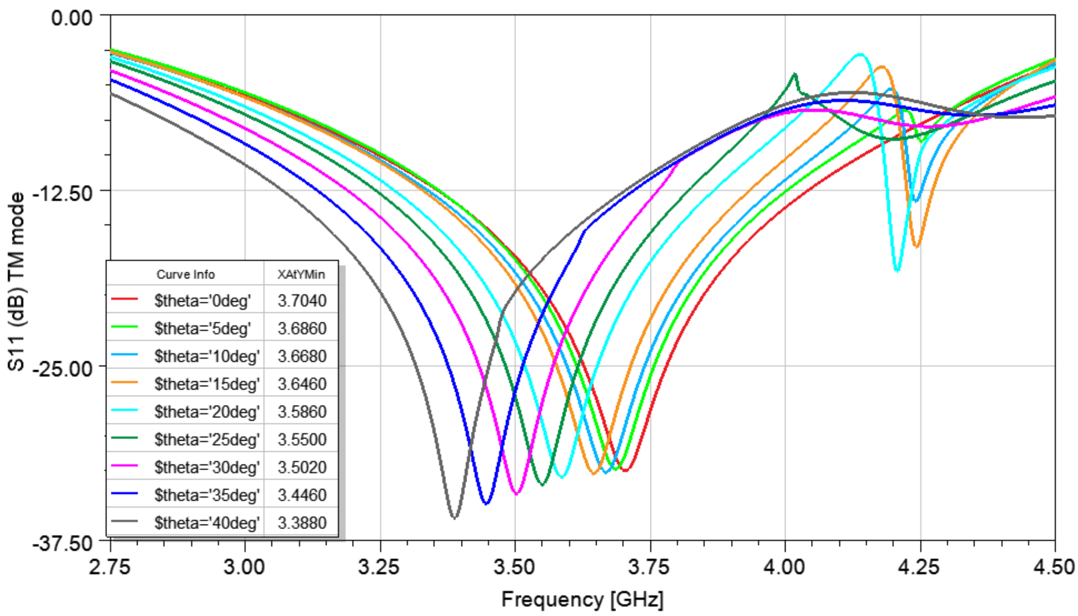

Figure 8.9 : Asymmetrical double circle loop S_{11} results for different incidence angle from 0º to 40º TM mode.

By comparing the results of asymmetrical design to the symmetrical one, we can see the it has a better performance in accordance to the second resonance created and linearity at the same (Table 8.2).

Table 8.2 : Values of center frequency of the double circle loop with asymmetrical dipoles with different angles in TM mode.

Degree (º)	Frequency (GHz)	Deviation (%)
0	3.702	0
5	3.686	0.432
10	3.668	0.918
15	3.646	1.512
20	3.586	3.133
25	3.550	4.105
30	3.502	5.402
35	3.446	6.915
40	3.388	8.481

Figure 8.10, Figure 8.11, and Figure 8.12 show how the frequency response at different angles changes when the inner circle gets close or far away from the outer circle loop, where this is mainly determined by adjusting the (R1) value.

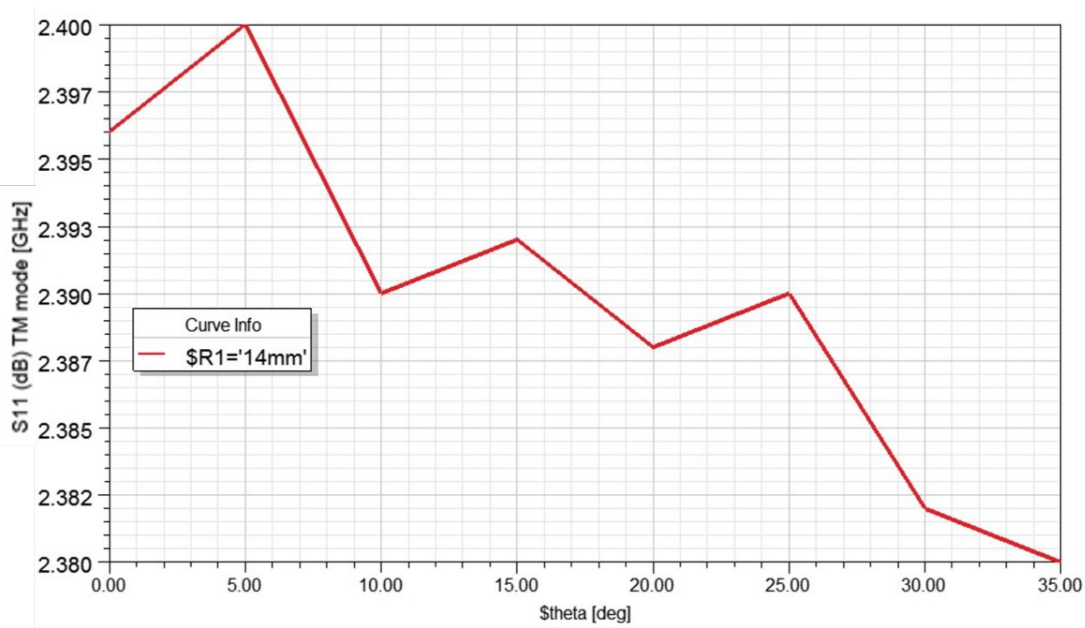

Figure 8.10 : Asymmetrical double circle loop S_{11} response for different incidence angle from 0º to 35º TM mode for R1 = 14 mm.

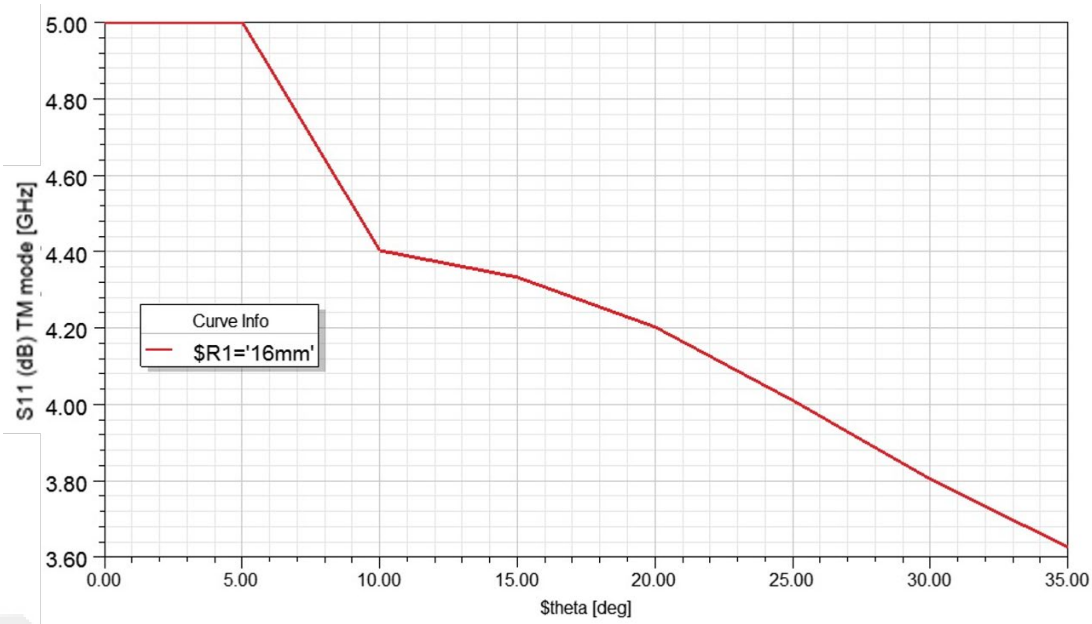

Figure 8.11 : Asymmetrical double circle loop S_{11} response for different incidence angle from 0º to 35º TM mode for R1 = 16 mm.

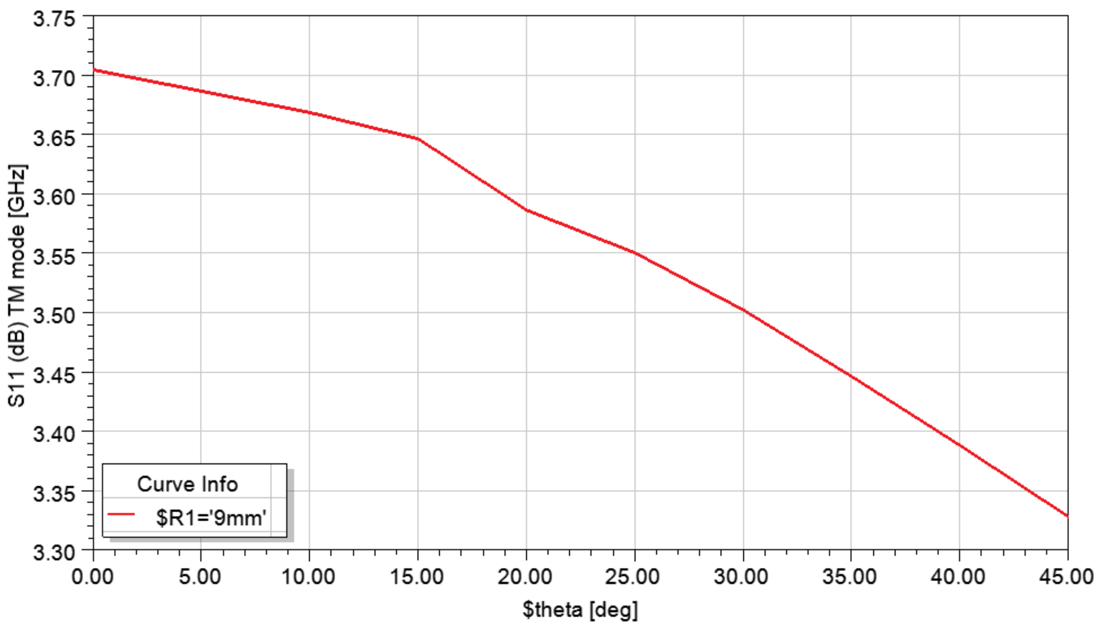

Figure 8.12 : Asymmetrical double circle loop S_{11} response for different incidence angle from 0º to 40º TM mode for g = 9 mm.

We can notice that when the inner circle gets closer to the outer one the linearity of the frequency response breaks down as in Figure 8.10 the frequency response is going up and down and in Figure 8.11 the frequency response is stable and not changing from zero to five degree. While in Figure 8.12 we can see that how the frequency response is changing linearly.

Where an illustration of TE and TM incidence with direction of propogation (DOP) are explained in Figure 8.13.

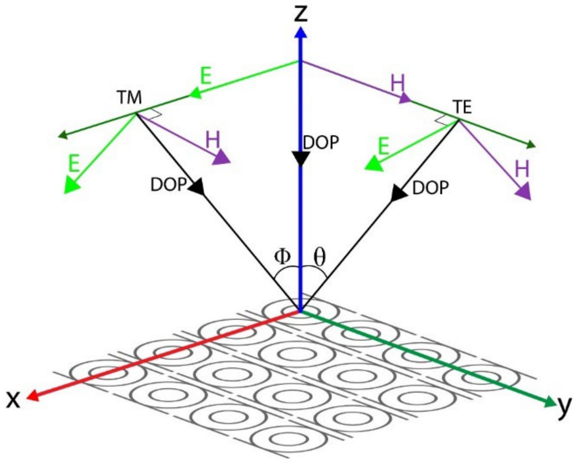

Figure 8.13 : Illustration of TM and TE on our asymmetrical design.

8.2 Design of FSS as a Passive Sensor Based on Crossed Shape Element for Crack Detection

Fundamentally, when FSS is used as a passive sensor to detect mechanical strain or cracks this will be based on the resonance frequency shift affiliated with a geometrical shape change of the FSS element. So, when a deformation or a crack in the structure occurs. Where, the resonance frequency will be changed by the effective length increase of the FSS element in the presence of a strain in the structure. Furthermore, when the structure is damaged, cracks from structural damage can cut the FSS element length and leave a gap. For this reason, a cross shaped FSS element were designed to detect cracks in civil structures (Figure 8.14)

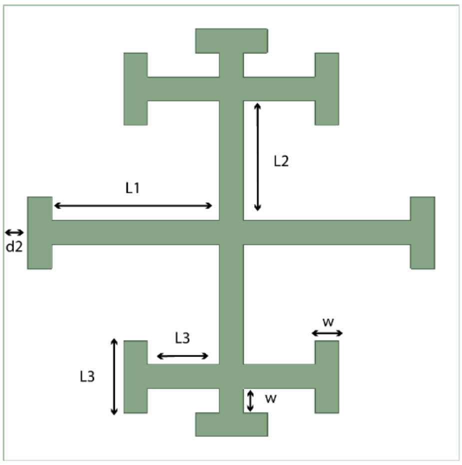

Figure 8.14 : Cross Shape Element.

For this reason, a cross shaped FSS element were designed to detect cracks in civil structures (Figure 8.14) where the parameters studied are L1= 14 mm, L2 = 10 mm, L3 = 6 mm, W = 2 mm and d2 = 2 mm. We know that the resonance frequency is defined according to many factors, one of them is the size and the length of the unit cell, where the original unit cell size and length were designed to work in S band. Figure 8.15 shows how the current is flowing and as we can see the right and left arms of the shape they are operating as passive elements and they won't have that much effect on the frequency response, where Figure 8.16 represents the frequency response in TM mode and Figure 8.17 represents the frequency response in TE mode before the crack occurs.

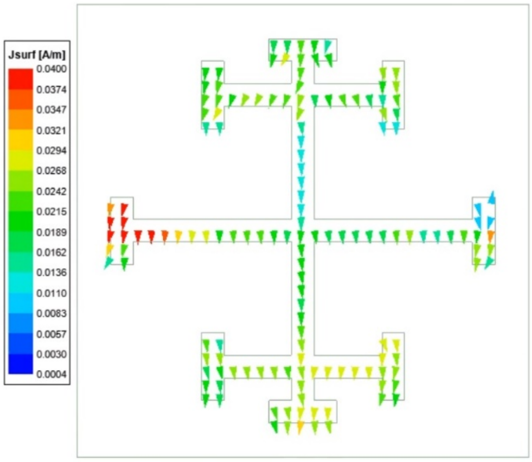

Figure 8.15 : Current flow and direction of Cross Shape Element.

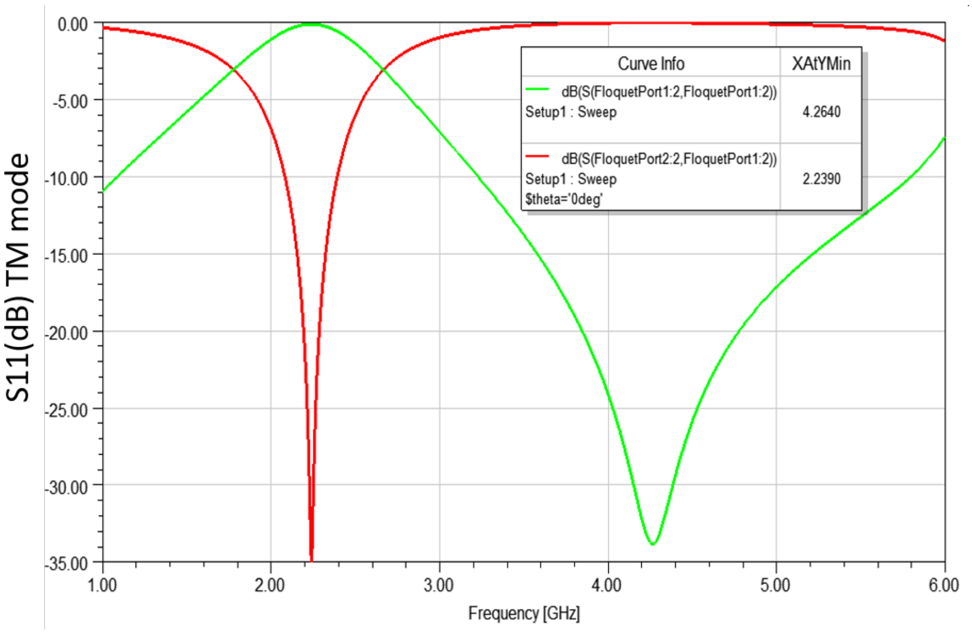

Figure 8.16 : Frequency response before cracking in TM mode.

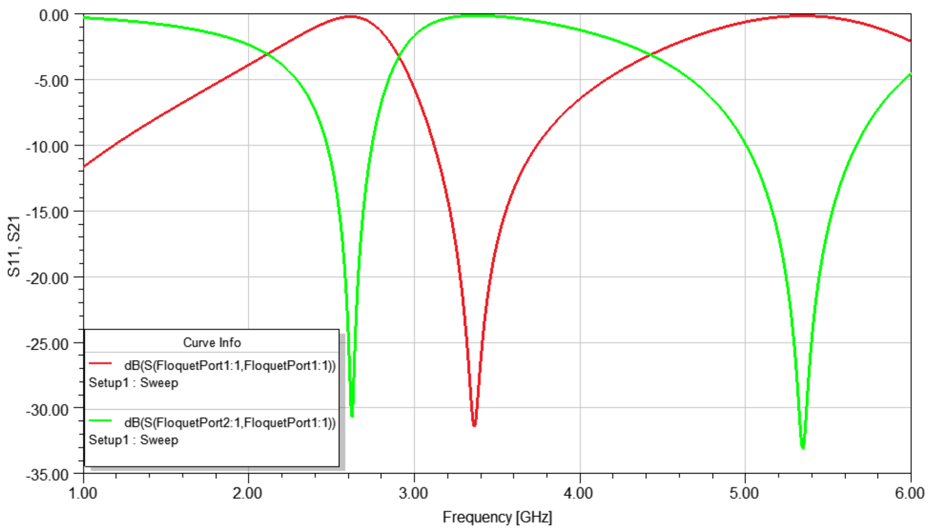

Figure 8.17 : Frequency response before cracking in TE mode.

But when the crack occurs anywhere in the upper side (Figure 8.18), where the crack is represented with X and it cracks L2 into L4 and L5, the frequency response will be altered and changed. As we can see, when the current can't go any further it changes its way and it goes to the right and left arms, where here the importance of the right and left arms arises. Another important thing is adding the small dipoles to the upper and lower side of the design, these dipoles ensure creating a second resonance frequency.

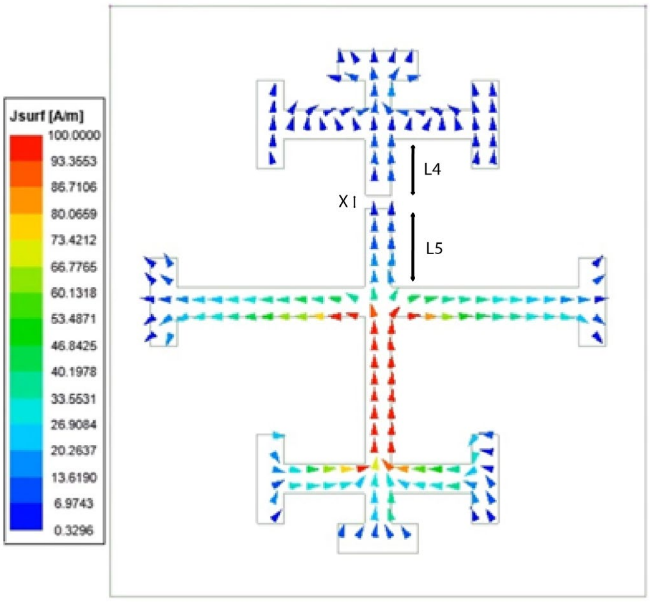

Figure 8.18 : Current flow and direction of cracked Cross Shape Element.

As we can notice from Figure 8.19, the first resonance frequency after the cracks happens changes slightly, but comparing that with the second resonance we can see that the second one is changing in a better way and it makes the resonance bandwidth wider. The main reason of the first resonance is not changing that much is because after the cracks happens the current keeps floating to the right and left arms, where in total they will be having approximately the same length of the original unit cell before it cracks. The current changes its way when the crack occurred, that's because after the gap is created (X) the electrons now stored, so when a new one tries to move forward, they won't be able to do that so they change their way.

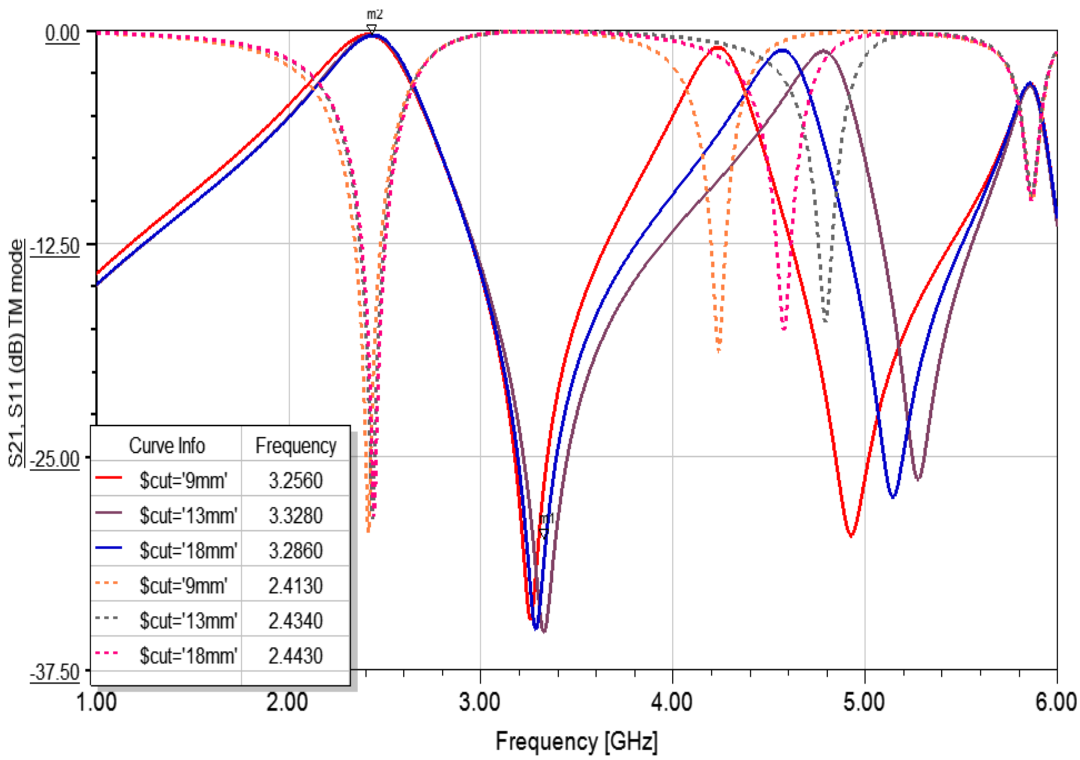

Figure 8.19 : Frequency response after cracking at different positions in TM mode.

From Figure 8.18, we can see that the crack (X) can happen at any point up between length L4 and L5, where the frequency response will change reasonably, and the current will keep moving towards the right and left arms. Here the importance of the arms arises, where when they are removed the frequency response will change differently and it will be hard to understand that.

Also, from Figure 8.18 we considered the crack in the geometry to be X value, where this value may change according to many factors, such as the force applied on the geometry. Therefore, Figure 8.20 shows the frequency response of different crack (X) thicknesses, where if we compared the frequency response with one before cracking (Figure 8.17) we can see how the frequency response is changing.

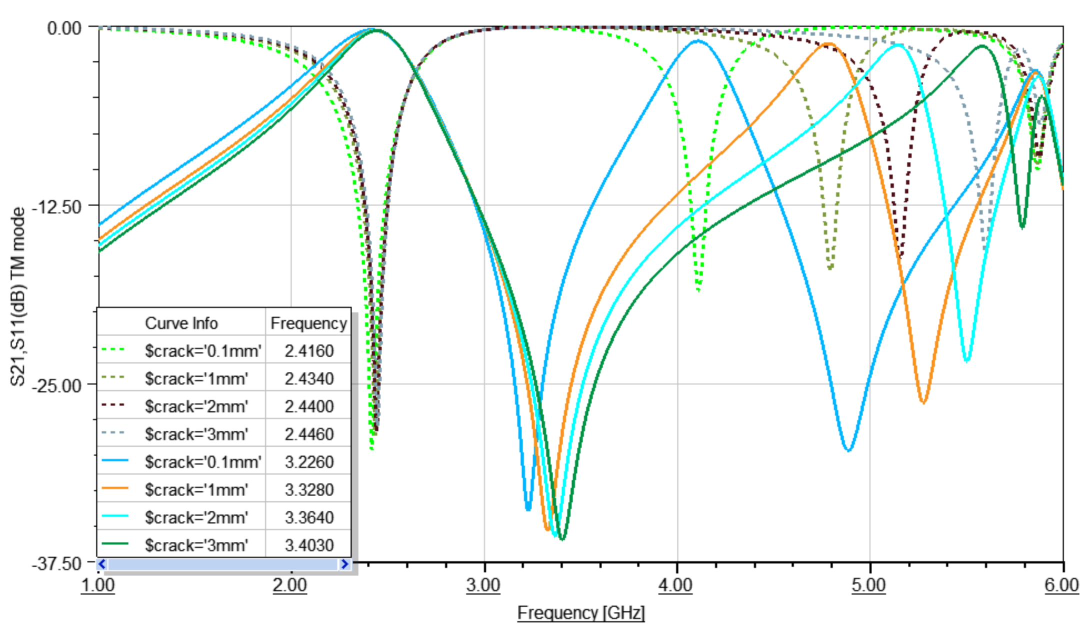

Figure 8.20 : Current flow when the crack happens in the right or left arms.

All discussed above is when the crack occurs along the x-axis, Figure 8.21 shows the current flow when the crack occurs along the y-axis. As we can see the current flows along the y-axis with the direction of the electric field.

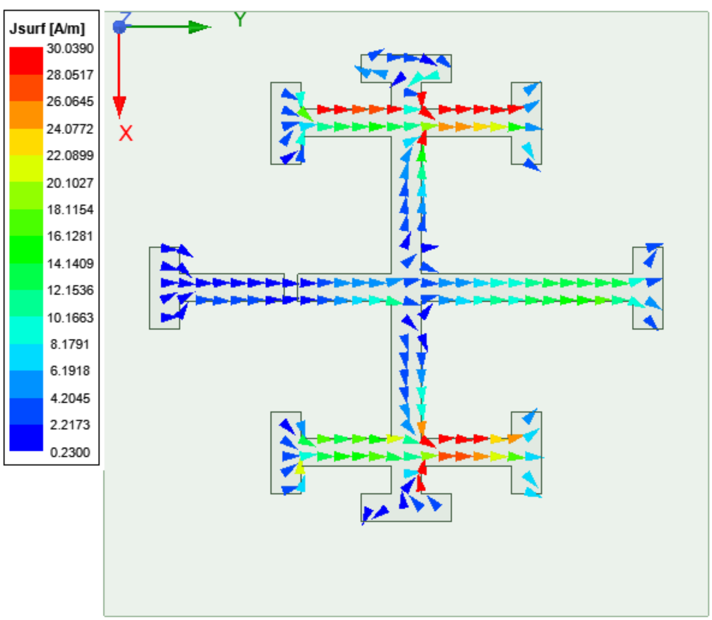

Figure 8.21 : Current flow when the crack happens in the right or left arms.

Figure 8.22 represents the frequency response in different positions along the right and left arms in TE mode because as shown in Figure 8.21 the current traveling in the direction of the electric field. Where the frequency response in Figure 8.22 represented as solid lines refers to S_{11} and the ones represented as short dashes refer to S_{21}.

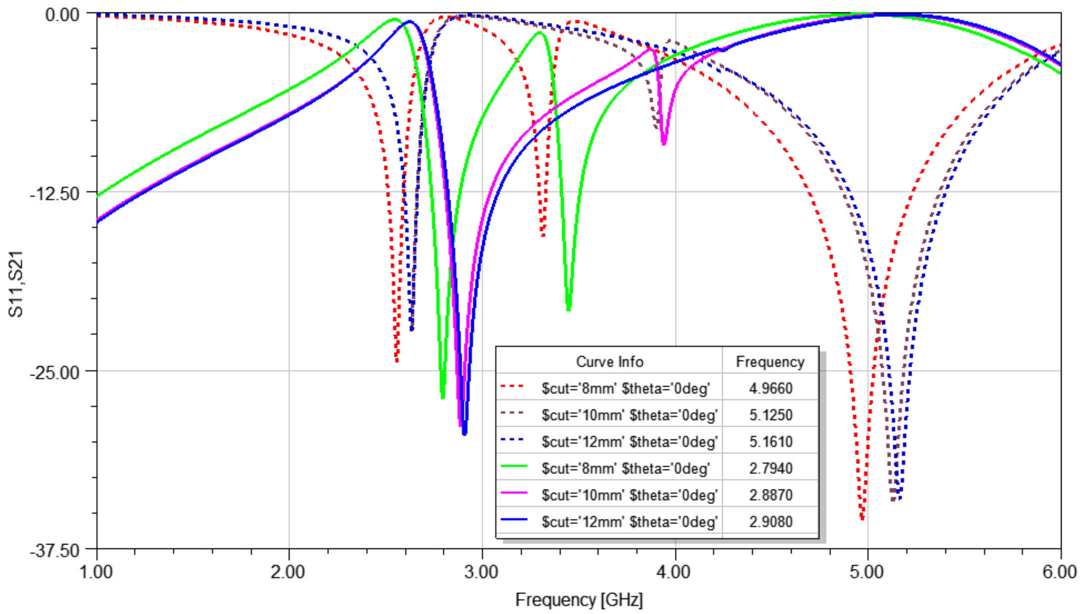

Figure 8.22 : Frequency response after cracking at different positions in TE mode.

9. CONCLUSION AND RECOMMENDATIONS

In this thesis, structural health monitoring using FSS as a passive sensor is applied to detect two type of deformations that might happen to a civil structure. The first deformation type is detecting tilting in structure, the performance and simulations of our design detects deviations for every 5-degree incident angle changing in a linear aspects in the reflected mode.

The second deformation type, is detecting normal strain and cracks in civil structures, the performance and simulations are presented that from the frequency response we can identify crack with different thickness and different positions. Additionally, the two proposed designs can be printed and tested on a civil structure and the results can be compared to the simulations represented in future work.

REFERENCES

[1] **B. A. Munk.** (2000). *Frequency selective surfaces theory and design,* New York: Wiley-Interscience.

[2] **A.K. Rashid, B. Li, Z. Shen.** (2014). An Overview of Three-Dimensional Frequency-Selective Structures. IEEE Antennas and Prop. Magazine, Vol. 56, Iss. 3, June, pp. 43-67.

[3] **T.K. Chang, R.J. Langley, E.A. Parker.** (1996). Active Frequency-Selective Surfaces, *IEE Proceedings, Microwaves, Antennas, and Propagation, Vol. 143, Iss*. 1, Feb.

[4] **F. Costa, A. Monorchio, G. Manara.** (2010). Analysis and Design of Ultra-Thin Electromagnetic Absorbers Comprising Resistively Loaded High Impedance Surfaces*, IEEE Trans. on Antennas and Prop., Vol. 58, Iss. 5, Mar. pp. 1551-1558.*

[5] **J. Romeu, Y. Rahmat-Samii.** (2000). Fractal FSS: A Novel Dual-Band Frequency Selective Surface, *IEEE Trans. on Antennas and Prop., Vol. 48, Iss. 7, Jul. pp. 1097-1105.*

[6] **Anwar, R., Mao, L. and Ning, H.** (2018). Frequency Selective Surfaces: A Review. Applied Sciences, 8(9), p.1689.

[7] **G. V. Eleftheriades and K. G. Balmain.** (2005). Negative-Refraction Metamaterials: Fundamental Principles and Applications, John Wiley and Sons.

[8] **T. K. Wu.** (1995). Frequency Selective Surface and Grid Array, John Wiley & Sons.

[9] **R. Ulrich.** (1967). Far-infrared properties of metallic mesh and its complementary structure*, Infrared Physics, vol. 7, no. 1, pp. 37-55.*

[10] **E. Pelton and B. Munk.** (1979) Scattering From Periodic Arrays of Crossed Dipoles, *IEEE Trans. on Ant. and Propag., Vol. 27 (No. 3), p. p. 323-330.*

[11] **G.J. Cox , K. Zorzos , R.D. Seager , J.C. Vardaxoglou.** (2001). Study of frequency selective surface (FSS) resonator elements on a circular dielectric rod antenna for mobile communications, *IEEE 11th International Conference on Antennas and Propagation(ICAP 2001), vol.2 no.480, p. p. 758-761.*

[12] **B. Hooberman.** (2005). Everything you ever wanted to know about frequency-selective surface filters but were afraid to ask.

[13] **P. Callaghan, E.A. Parker, and R.J. Langley.** (1991). Influence of Supporting Dielectric Layers on the Transmission Properties of Frequency Selective Surfaces, *Microwave, Antennas, and Prop. IEEE Proceedings H, Vol 138, no. 5, Oct. pp. 448-454.*

[14] **C. C. Chen.** (2005). Transmission through a conducting screen perforated periodically with Cambridge: Cambridge University Press.

[15] **D. B. Davidson.** Computational Electromagnetics for RF and Microwave Engineering.

[16] **I. Bardi, R. Remski, D. Perry and Z. Cendes.** (2002). Plane wave scattering from frequency selective surfaces by the finite-element method. *IEEE Transactions on Magnetics, 38(2), 641-644.*

[17] **A. Taflove and K. R. Umashankar.** (1989). Review of FDTD numerical modeling of electromagnetic wave scattering and radar cross section, *Proc. IEEE, vol. 77, no. 5, pp. 682-699.*

[18] **B. A. Munk.** (1985) On stabilization of the bandwidth of a dichroic surface by use of dielectric slabs. *Electromagnetics, vol. 5, no. 4, pp. 349-73*.

[19] **R. J. Langley and E. A. Parker.** (1982). Equivalent circuit model for arrays of square loops. Electronics Letters, 18(7), 294-296.

[20] **C. K. Lee and R. Langley.** (1985). Equivalent-circuit models for frequency selective surfaces at oblique angles of incidence. Paper presented at the IEE Proceedings H (Microwaves, Antennas and Propagation).

[21] **N. Marcuvitz.** (1951). *Waveguide handbook*: Iet

[22] **A. E. Yilmaz and M. Kuzuoglu**. (2009). Design of the square loop frequency selective surfaces with particle swarm optimization via the equivalent circuit model. *Radioengineering, 18*(2), 95-102.

[23] **A. Hamdan, M.T.H Sultan, F. Mustapha.** (2019). Structural Health Monitoring of Biocomposites, *Fibre-Reinforced Composites and Hybrid Composites, pp. 227-24.*

[24] **Fa-Hwa Cheng, Initials.** (1997). Strength of material. Ohio: McGraw-Hill Mechanics of Materials, E.J. Hearn.

[25] **Shear Strain.** (2020) *School of Materials Science and Engineering*. ,2020. Retrieved: Feb 26, 2020, from http://www.materials.unsw.edu.au/tutorials/online-tutorials/5-shear-strain.

[26] **Lecture Notes** *Universiti Malaysia Pahang*. Retrieved: Feb 26, 2020, from: http://ocw.ump.edu.my/pluginfile.php/17228/mod_resource/content/1/CHAPTER%209.pdf.

[27] **S. Safri, M. Sultan and M. Jawaid.** (2019). Damage analysis of glass fiber reinforced composites. *pp. 133-147*.

[28] **Pieper, Dustin F., and Kristen M. Donnell.** (2015). Application of frequency selective surfaces for inspection of layered structures. *Instrumentation and Measurement Technology Conference (I2MTC), 2015 IEEE International. IEEE.*

[29] **Pieper, Dustin F., and Kristen M. Donnell., Abdelkarim, Omar., A. ElGawad, Mohamed.** (2016). Embedded FSS Sensing for Structural Health Monitoring of Bridge Columns, *Instrumentation and Measurement Technology Conference I2MTC, IEEE International. IEEE.*

[30] **E.A. Parker.** (1991). The Gentleman's Guide to Frequency Selective Surfaces. *Q.M.W. Antenna Symposium, London, U.K.*

[31] **B.J. Arritt, A.F. Starr, D.R. Smith.** (2009). Electromagnetic Performance of Mechanically Loaded Composite Metamaterials. *International Conference on Composite Materials (ICCM) 17.*

[32] **B. Arritt, B. Adomanis, T. Khraishi, D. Smitt.** (2010). Parametric Analysis of the Strain-Dependant Behavior of a Metamaterial Electric Resonantor. *App. Physics Letters, Vol. 97, Iss. 19.*

[33] **R. Melik, E. Unal, N.K. Perkgoz, C. Puttlitz, H.V. Demir.** (2009). Flexible Metamaterials for Wireless Strain Sensing. *App. Physics Letters, Vol. 95, Iss. 18.*

[34] **S.D. Jang, B.W. Kang, J. Kim.** (2013). Frequency Selective Surface Based Passive Wireless Sensor for Structural Health Monitoring. *Smart Materials and Structures, Vol. 22, No. 2.*

[35] **Mechanics of Materials: Strain, Mechanics of Slender Structures**. (2020) Boston University, Retrieved: Feb 26, 2020 from https://www.bu.edu/moss/mechanics-of-materials-strain.

[36] **B.J. Arritt, A.F. Starr, D.R. Smith.** (2009). Electromagnetic Performance of Mechanically Loaded Composite Metamaterials. *International Conference on Composite Materials (ICCM).*

[37] **E. Kinzel, K. Donnell, K. Chandrashekhara.** (2014). Structural Health Monitoring and Remote Sensing of Transportation Infrastructure Using Embedded Frequency Selective Surfaces. *Missouri S&T, Rolla, MO, Tech. Rep. NUTC R365.*

[38] **Strain gauge measurements**. (1998). International instruments, Retrieved: March 03, 2020, from http://elektron.pol.lublin.pl/elekp/ap_notes/NI_AN078_Strain_Gauge_Meas.pdf .

[39] **E. Kinzel.** (2014). Design of a Frequency-Selective Surface Strain Sensor. *IEEE APS, Memphis, TN, pp. 2074-2075.*

[40] **P. Bevelacqua.** *The Antenna Theory Website*. Retrieved: March 09, 2020 from http://www.antenna-theory.com.

[41] **O. Abdelkarim, A. Gheni, S. Anumolu, S. Wang, M. ElGawady.** (2015). Hollow-Core FRP-Concrete-Steel Bridge Columns under Extreme Loading. *Missouri S&T, Rolla, MO. Tech. Rep. cmr 15-008.*

[42] **A. Foudazi, K.M. Donnell, M.T. Ghasr.** (2014). Application of Active Microwave Thermography to Delamination Detection. *Proceedings of the International Instrumentation and Measurement Technology Conference (I2MTC), Montevideo, Uruguay, pp. 1567-1571.*

[43] **Martin Barth, Frank Schubert, and Bernd Koehler.** (2008). Where X-ray imaging fails – delamination, crack, and micro-pore detection using ultrasonic reflection tomography in a scanning acoustic microscope. *Nuclear Science Symposium (NSS), Dresden, Germany, pp. 577-581*.

PUBLICATIONS/PRESENTATIONS ON THE THESIS

- Başoğlu M., Döken B., and Pınar S., 2020: Using Frequency Selective Surface as a Passive Sensor in Structural Health Monitoring. *2nd Hezarfen International Science, Mathematics and Engineering Sciences Congress*, September 25-26, 2020 Antalya, Turkey.